12-5-2017 11:00 AM

A Comparison between Different Snubbers for Flyback Converters

Adel Alganidi, *The University of Western Ontario*

Supervisor: Moschopoulos, Gerry, *The University of Western Ontario*

A thesis submitted in partial fulfillment of the requirements for the Master of Engineering Science degree in Electrical and Computer Engineering

Abstract

The DC-DC flyback power converter is widely used in low power commercial and industrial applications (> 150 W) such as in computers, telecom, consumer electronics because it is one of the simplest and least expensive converter topologies with transformer isolation. Its main power circuit consists of just a semiconductor device like a MOSFET operating as a switch, a transformer, an output diode and an output filter capacitor. The converter switch, however, is susceptible to high voltage spikes due to the interaction between its output capacitance and the leakage inductance of the transformer. These spikes can exceed the ratings of the switch, thus destroying the device, and thus flyback converters are always implemented with some sort of snubber circuit that can clamp any voltage spikes that may appear across their switches.

There are two types of snubbers: passive snubbers that consist of passive electrical components such as capacitors, inductors and diodes and active snubbers, that consist of passive components and an active semiconductor switch. It is generally believed that passive snubbers are less expensive but also less efficient than active snubbers, but this belief has been placed in doubt with recent advances in passive snubber technology. Flyback converter with regenerative passive snubbers that dissipate little energy have been recently proposed and have greater efficiency than traditional passive snubbers. Although the efficiency of passive snubbers has improved, no comparison has been made between these new passive snubbers and active snubbers as it is still assumed that active snubbers are always more efficient.

The main focus of this thesis is to compare the performance of an example passive snubber and an example active snubber. These example snubber circuits have been selected as being among the best of their types. In this thesis, the steady-state operation of each snubber circuit is explained in detail and analyzed, the results of the analysis is used to create a procedure for the design of key components, and the procedure is demonstrated with a design example. The results of the design examples were used to build prototypes of flyback converters with each example snubber and the prototypes were used to obtain experimental results. Based on these experimental results, conclusions about the efficiency of flyback converters with passive

regenerative and active snubbers operating under various input line and output load conditions are made in this thesis.

Acknowledgement

I would like to express my sincere gratitude to my supervisor, Prof. Gerry Moschopoulos, for his invaluable supervision , encouragement. His guidance kept me on track during my studies and his advice to me was invaluable.

I would also like to acknowledge financial support from the Ministry of Education of Libya for this work.

Western University has been the ideal setting for the past two years of study and I would like to acknowledge the many selfless acts of faculty and staff, which have culminated into a productive and memorable university experience.

Part of this research was performed in the epower Lab of Queens University, and I would like to thank all my colleagues there. I am greatly obliged to Mr. Behnam Koushki for his technical support. I also would like to say thank you to Amit Kumar, Omid Salari, Hamid Reza etc. for their support.

I would like to thank Mr. Adel Abosnina for his support at Western University.

Lastly, I would like to thank my family back home country who helped me to grow up in a highly supportive and environmentally conscious atmosphere. I am forever indebted to my parents who have been a constant source of inspiration throughout my life.

Table of Contents

List of tables

List of Figures

Nomenclature

AC	Alternating current
CCM	Continuous condition mode
C_{clamp}	Clamp capacitor (F)
C_o	Filter capacitor (F)
$\mathbf{C_r}$	output capacitor of MOSFET
D	Duty cycle
DC	Direct current
D_{o1}	Output rectifier
D_{on}	On-time for the switch
D_{reg}	Diode in the regenerative branch
ESR	Equivalent series resistance (Ohm)
f_{sw}	Switching frequency (Hz)
I_{ds}	Current through the channel of MOSFET (A)
$I_{L_{m,max}}$	Maximum current through magnetizing inductance (A)
$I_{L_{m,min}}$	Minimum current through magnetizing inductance (A)
$I_{Lik_{min}}$	Minimum current through leakage inductance (A)
$I_{Cclamp,peak}$	Peak current through clamp capacitor (A)
ΔI_{L_m}	Ripple current in magnetizing inductance
L_{ik}	Leakage inductance
L_m	magnetizing inductance (H)
LCDD	Inductor, capacitor, and two diodes
L_r	Resonant inductor (H)

MOSFETs	Metal oxide semiconductor field effect transistors
N_P	Primary turns
N_s	Secondary turns
N_t	Territory turns
n_t	Turns ratio territory to primary
n_s	Turns ratio secondary to primary
P_o	Output power (W)
PWM	Pulse width modulation.
$R_{DS(on)}$	Resistance between drain and sources of MOSFET during on-state (Ohm)
R_{sn}	Snubber resisitor
RCD	Resistor, capacitor, and diode
RMS	Root mean square
S_{main}	Main switch
S_{aux}	Auxiliary switch
T_{main}	Main transformer
Δt	Time variation (Sec)
T_s	Duration of one cycle (Sec)
V_{clamp}	The voltage across the clamp capacitor
V_{fw}	Voltage drop across diode in forward-biased (V)
$V_{D_{o1,rev,max}}$	Maximum reverse voltage across the output rectifier
V_{ds}	Voltage between drain and source of MOSFET (V)
V_{in}	Input voltage (V)
V_o	Output voltage
ΔV	Voltage variation (V)
V_o	Output voltage (V)

ω	Angular frequency
Z	Characteristic impedance (Ohm)
ZCS	Zero current switching
ZVS	Zero-voltage switching
η	Efficiency

Chapter 1

1 Introduction

1.1 Power Electronics

Power electronics is the branch of electrical engineering that studies the use of electronics to convert power from the form supplied by a source to the form required by a load. Power converters are widely used because it is rare for an available power source such as an AC outlet, solar panel, or battery, to match the requirements of a load such as a motor, a desktop computer, or telecom equipment. They typically consist of semiconductor devices such as diodes and transistors used as on/off switches, magnetic elements such as inductors and transformers, and capacitors. As there are two general types of sources, AC and DC, and two general types of loads, AC and DC, therefore, there are four general types of power converters: AC-DC, DC-DC, DC-AC, AC-AC. The focus of this thesis is on low power DC-DC converters.

1.2 MOSFETS

For such applications, MOSFETs (metal-oxide-semiconductor field-effect transistors) are used as the converter switches as they can turn on and off quickly and are inexpensive. MOSFETs can be either N-channel or P-channel as shown in Fig. 1.1(a) and Fig. 1.1(b) respectively; N-channel MOSFET are preferred as they can handle more voltage and current stress. An N-channel MOSFET operates as follows: When sufficient voltage is placed across its gate and source, a channel opens up in the device and current flows from drain to source; current stops flowing in the device after the gate-source voltage is removed. A MOSFET can be considered to consist of a switch, an anti-parallel diode and a drain-source capacitor, as shown in Fig. 1.2. When the switch is on, the device has an equivalent resistance of $R_{DS(on)}$ across its drain-source terminals.

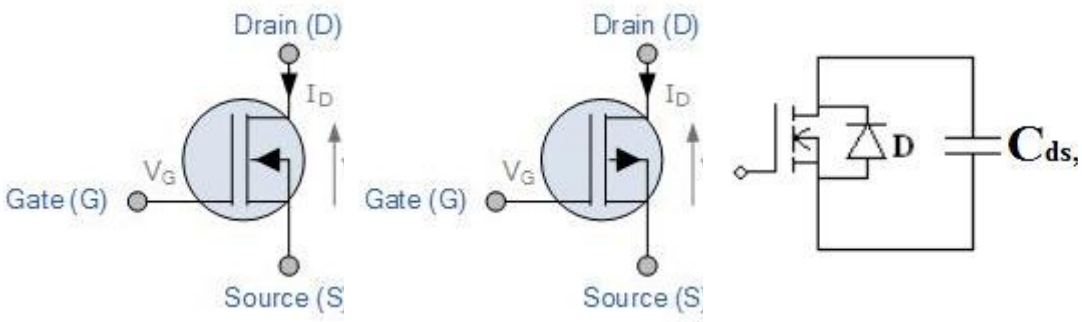

(a) (b) (c)

Fig. 1.1 (a) N-channel MOSFET. (b) P-Channel MOSFET. (c) Equivalent MOSFET model

An ideal MOSFET device would not dissipate any power when in operation. Such a device does not exist in the real world and a MOSFET does have power losses. These losses can be classified as being either conduction losses or switching losses. Both types are reviewed here.

Conduction losses are caused whenever current flows from drain to source in a MOSFET. Since a MOSFET can be considered to be a resistor when it is fully on and operating as an on/off switch, power is lost when current is flowing through the device and as when current is flowing through a resistor.

Switching losses are caused whenever a MOSFET undergoes a switching transition, either when it is turned on or it is turned off. The power losses are caused by the overlap between the voltage across the switch and the current flowing through it as power is related to the product of voltage and current. This overlap can be seen in the drain-source voltage (V_{ds}) and drain current (I_{ds}) waveform shown in Fig. 1.2; it should be noted that the overlaps of voltage and current have been exaggerated. From these waveforms, it can be seen that the rise and fall of voltage and current is not instantaneous as the edges of both waveforms are not sharp. In an ideal switching device, both waveforms would be perfect rectangles and there would be no overlap between the two waveforms.

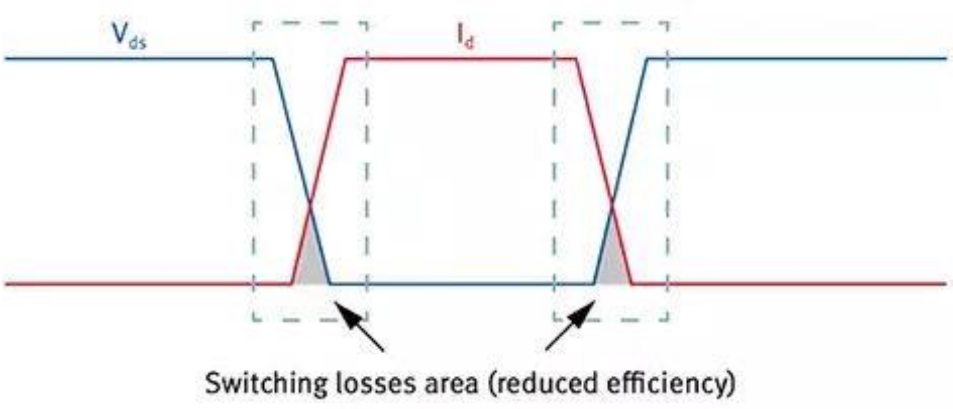

Fig. 1.2 Switching losses of a non-ideal MOSFET.

1.3 Flyback Converters

The components of a power electronic converter can be arranged in many ways to form electrical circuit structures; such structures are referred to as topologies in the literature. For low power DC-DC converters, the most popular topology for DC-DC conversion applications involving 150 W of power or less is the flyback converter because of its cost and simplicity. A circuit diagram of the standard DC-DC flyback converter is shown in Fig. 1.3.

As can be seen from Fig. 1.3, the converter consists of a MOSFET device that is used as a switch, a transformer, a diode, and a capacitor. The converter operates as follows: When the MOSFET switch is turned on, voltage is impressed across the primary of the transformer and energy is stored in the transformer. No energy is transferred to output during this time as the output diode is reverse-biased due to the polarity of the transformer secondary and the way it is connected to the diode; energy is supplied to the load by the output capacitor. When the switch is turned off, current stops flowing in the transformer's primary and polarity of the transformer's secondary voltage changes so that the output diode becomes forward-biased and current flows to the output. It is during this time that energy is transferred from the transformer to the output.

The switch is turned on and off in a periodic manner. For a given set of component parameters, the amount of output DC voltage is determined by how long the switch is on during a switching cycle (period) – the longer the switch is on, more output DC voltage is generated. Time must be allowed, however, for the transformer to be reset

so that the negative volt-seconds (defined as the amount of voltage over a given time) placed across a transformer is equal to the positive volt-seconds. If this condition is not satisfied, then more energy will be placed in the transformer than will be removed during a switching cycle so that the net accumulation in energy will result in the transformer becoming saturated and the transformer primary becoming a short-circuit. The result of this short-circuit will be a catastrophic failure of the switch due to excessive peak current.

It should be noted that flyback converters, like most DC-DC converters in general, are operated with high switching frequencies (> 25 kHz) as this reduces the size of the transformer and the output capacitor. Doing so is advantageous as smaller power converters in electrical equipment or consumer products result in their being more compact and the cost and size savings can be used to offer more features. Higher switching frequencies, however, also result in greater switching losses and less converter efficiency so that a compromise between converter size and efficiency must be considered.

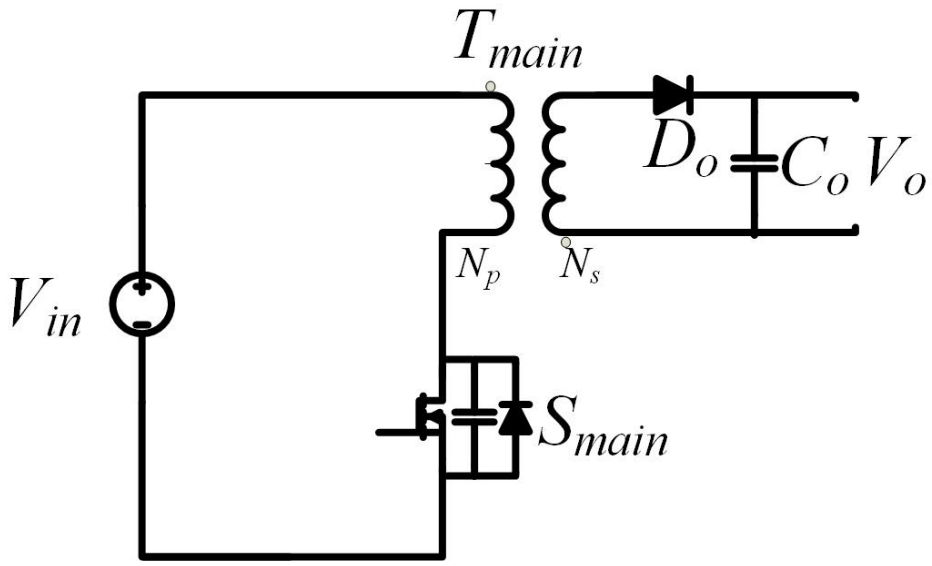

Fig. 1.3 Flyback converter.

1.3.1 Flyback Transformer with Leakage Inductance

A transformer in a flyback converter is generally a magnetic core with a primary winding and a secondary winding. Each winding is a wire wrapped numerous times around a magnetic core. Voltage can be stepped down or up depending on the number of turns of the secondary winding relative to those of the primary winding. When voltage is placed across the primary winding, magnetic flux is generated in the core with some leaking out in the air. Flux flowing through the secondary winding induces a voltage to appear across the winding's terminals and the output diode is either forward-biased or reverse-biased, depending on whether the flux is increasing or decreasing.

Leakage flux can be modeled as a leakage inductance as shown in Fig. 1.4. If there was no leakage flux, then there would be no leakage inductance as all the flux would flow through the transformer core. The effect of leakage inductance on the operation of the flyback converter is to force voltage spikes to appear across the MOSFET switch when it is turned off.

Consider the simplified circuit section shown in Fig. 1.5. This circuit section shows an inductor in series with a MOSFET switch that is drawn as the simplified model shown in Fig. 1.1(c); this diagram can be considered to be equivalent to having transformer leakage inductance in series with a switch. When the switch is on, current can be considered to flow through the inductor and the switch; when the switch is turned off, energy in the inductor cannot just disappear and thus the inductor current must have a path to flow through. This is the case in the flyback converter when the switch is turned off – energy in the transformer core can be transferred to the output, but energy in the leakage inductance cannot be. What can happen is that the leakage inductance current starts to flow through the drain-source capacitance of the MOSFET, thus charging up the capacitor and increasing the voltage across the device. Depending on the amount of energy stored in the leakage inductance, which is related to the amount of leakage flux in the transformer, the voltage across the device may exceed the device's ratings and a catastrophic failure of the device would happen.

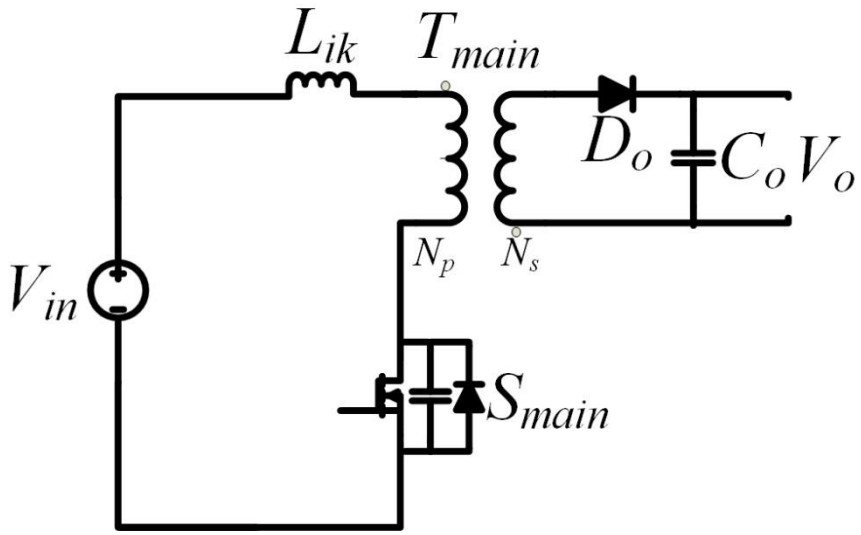

Fig. 1.4 Flyback converter with leakage inductance.

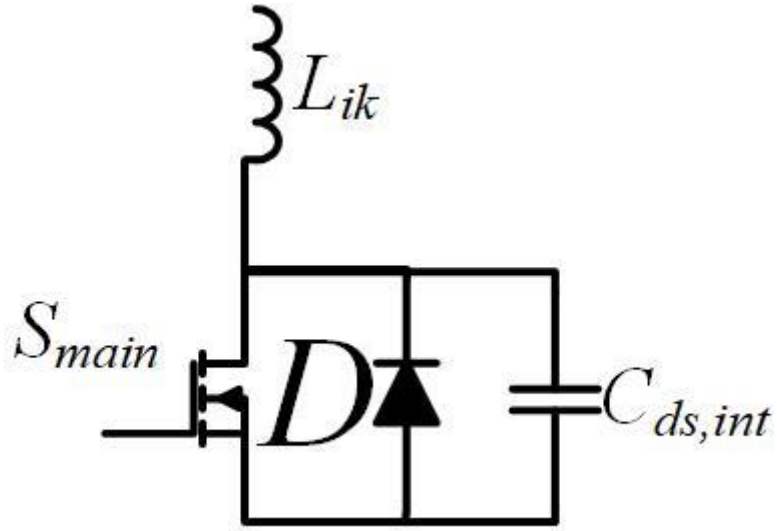

Fig. 1.5 Simplified flyback converter section with leakage inductance and switch.

1.4 Passive Snubber Circuits

The problem of excessive voltage spikes appearing across the flyback converter switch when it is turned off can be reduced if a passive snubber is added to the circuit. A passive snubber usually consists of a capacitor that is larger than the output capacitance of the switch and additional passive components that help discharge this capacitor; it gets its name from its ability to eliminate or “snub” voltage spikes. Adding a snubber increases the amount of capacitance seen by the leakage inductor, which slows down the rate of rise in voltage after the switch is turned off, thus

reducing any potential voltage spikes. A snubber also helps reduce turn-off switching losses as the slower rate of voltage rise during a turn-off transition reduces the amount of overlap between switch voltage and current during this transitions, which reduces the amount of power dissipated in the switch.

1.4.1 RCD Snubber

There are different types of passive snubber circuits. The simplest type is the RCD snubber circuit [1]-[7], which consists of a resistor, a capacitor, and a diode, as shown in a flyback converter in Fig. 1.6. The converter with the snubber works as follows: When the switch is turned off, the transformer's leakage inductance "sees" two possible current paths: one through the output capacitance of the switch and one through the snubber circuit capacitor C_{clamp}. As the net capacitance that is seen is larger than it would be without the RCD snubber in the circuit, the voltage rise across the switch is slower and the eventual switch voltage is less. Energy that is transferred to C_{clamp} is transferred to R_{sn}, which allows C_{clamp} to discharge so that its voltage does not become excessive.

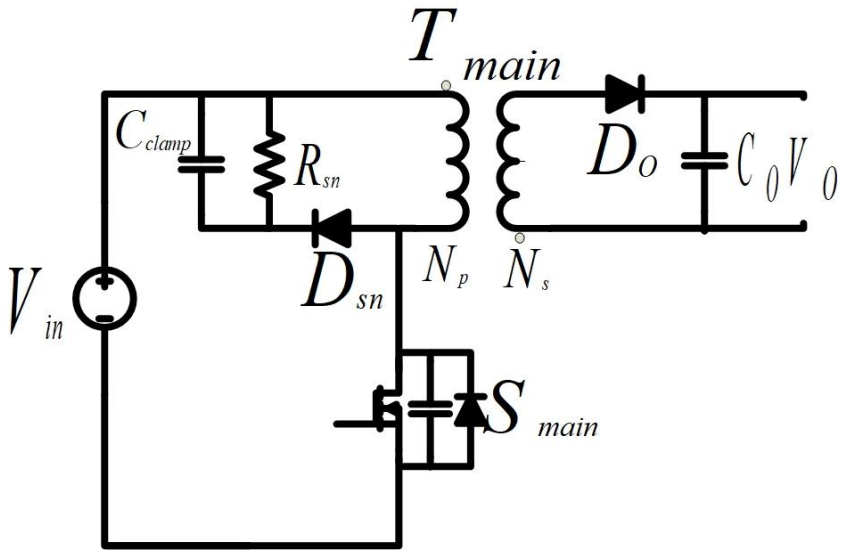

Fig. 1.6 Flyback converter with RCD snubber

1.4.2 LCDD Snubber

Although the RCD snubber can be effective in reducing switch voltage spikes, it is inefficient as all energy stored in the leakage inductance is dissipated through a resistor. An alternative passive snubber is the LCDD snubber [8] shown in a flyback converter in Fig. 1.7. This snubber consists of an inductor, a capacitor, and two diodes. The snubber works as follows: Like the RCD snubber, leakage inductor current flows through the output capacitance of the switch and the snubber capacitor when the switch is turned off. Some energy is transferred to the output during this time as a negative voltage is placed across the transformer primary. When the switch is turned on again, current flows through the switch from two paths, one from the transformer primary and one from C_{clamp}, diode D_2 and inductor $L_{auxiliary}$, thus discharging C_{clamp}. The circulating current that is the result of this second current path increases conduction losses and increases peak current stress in the switch. Although the LCDD snubber is more efficient than the RCD snubber, it is not considered to be an efficient snubber because not high portion of energy is recycled

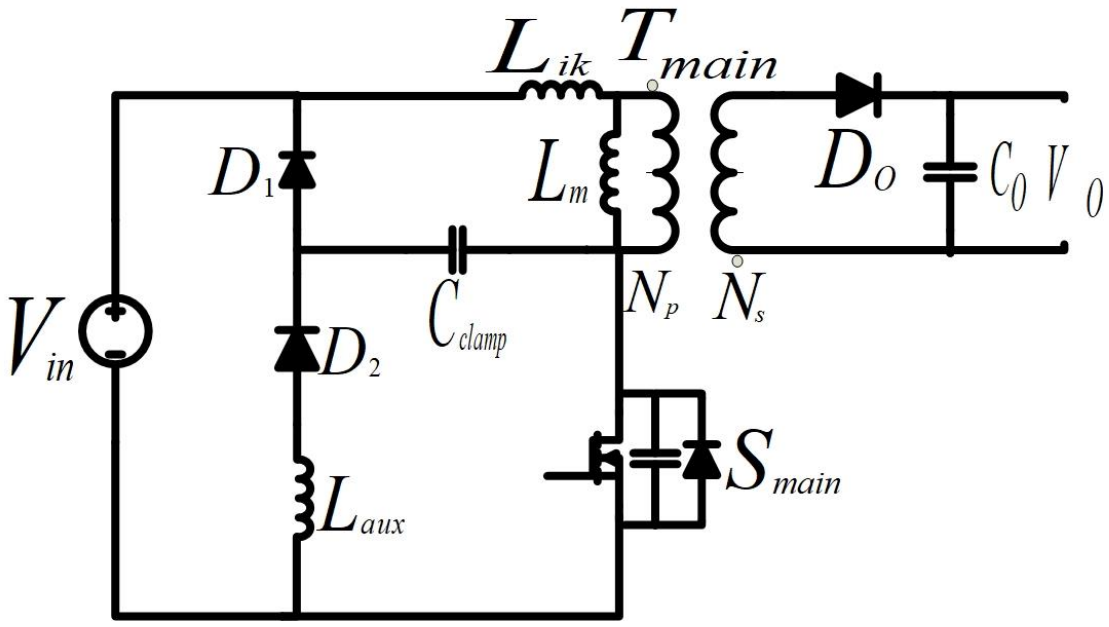

Fig. 1.7 A flyback converter with LCDD snubber.

1.4.3 Regenerative Energy Snubber

One type of passive snubber that is better than the RCD and LCDD snubbers is the regenerative snubber [9]-[13]. An example of a regenerative energy snubber in a flyback converter is shown in Fig. 1.8. This snubber is the same as the LCDD snubber with one important difference: the inductor in the LCDD snubber is replaced by a winding that is taken from the transformer. What this winding does is that it provides a way for more of the energy stored in C_{clamp} to be transferred to the output. It also provides a counter voltage to the voltage across C_{clamp} when the switch is turned on so that the amount of current that circulates through the switch is reduced, thus reducing conduction losses and peak current stresses. The operation of the converter shown in Fig. 1.8 is very similar to that of the LCDD snubber and thus it will not be explained here. Regenerative energy snubbers, so called because they do not dissipate energy like RCD snubbers, are considered to be the most efficient type of passive snubbers in the power electronics literature.

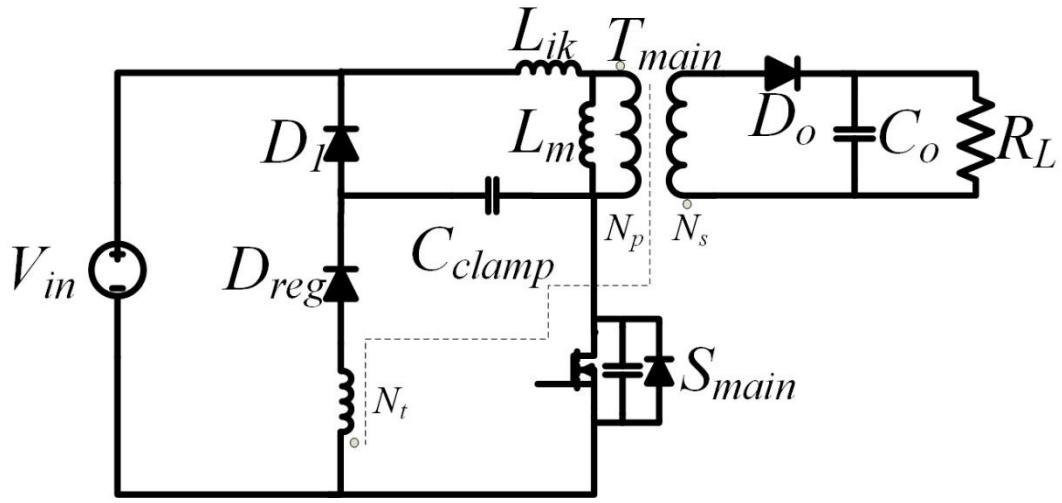

Fig. 1.8 A Flyback converter with a regenerative snubber.

1.5 Active Clamp Snubber

Passive snubbers can reduce switch turn-off losses because they reduce the overlap of voltage and current during the time a switch is turned off; they do nothing, however, to reduce turn-on losses. As a result, power electronics researchers have proposed various types of active snubbers that can do so [15-17].

An active snubber is a snubber that has an active switch in its circuit. This active switch allows the snubber to help reduce turn-on switching losses in addition to suppressing voltage spikes and reducing turn-off switching losses by allowing the main flyback converter switch to turn on with zero-voltage switching (ZVS). The term ZVS refers to any method that allows a converter switch to turn on with almost zero voltage across it during the turn-on switching transition time. Since the power dissipated in a switch during a switching transition is related to the product of the voltage across the switch and the current through it at the time of transition, making the switch voltage zero during this time ensures a significant reduction of switching losses as there is no overlap between voltage and current, given that there is no voltage.

A number of active snubbers have been proposed in the power electronics literature [14]-[19], but by far the most popular type is the active clamp snubber shown in a flyback converter in Fig. 1.9 [20-31]. This is because it is simple and inexpensive as it consists of an active switch and a clamping capacitor. The active clamp snubber is considered to be far superior to other active snubbers, which are used only under certain limited conditions such as limited input voltage range. Utilization of Active clamp for Forward converters are discussed in [32-37].

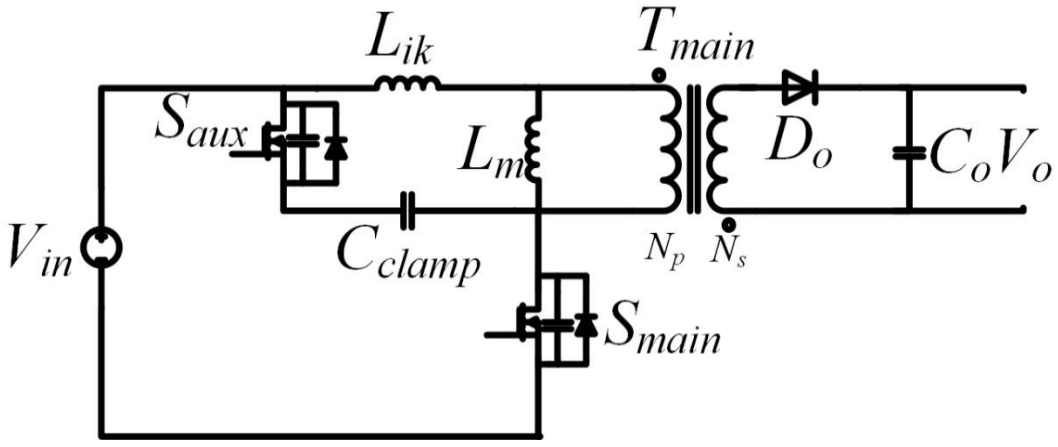

Fig. 1.9 Flyback converter with active clamp snubber.

1.6 Thesis Objectives

Passive snubbers are generally considered to be cheaper, but less efficient than active snubbers and the decision as to which type to use has mainly focused on cost. Recent advances in passive regenerative energy snubbers, however, have resulted in better efficiency for converters with passive snubbers than before so that while it was obvious in the past that active snubbers were always more efficient than passive snubbers, this is not so obvious now.

The best passive snubber is the regenerative energy snubber shown in Fig. 1.8 and the best active snubber is the active clamp snubber shown in Fig. 1.9. No comparison between these two snubbers has been reported in the power electronics literature and it is the main objective of this thesis to make such as comparison between these two snubbers for various input voltage and output load conditions. The results of the proposed research can be used by power electronics engineers to decide which snubber should be used, given a particular set of operating conditions.

1.7 Thesis outline:

This thesis is organized as follows:

In Chapter 2, the general operation of the regenerative energy snubber shown in Fig. 1.8 is explained in detail as are the modes of operation that a flyback converter with such a snubber goes through during a switching cycle. These modes of operation are analyzed and the results of the analysis are used to derive a procedure for the design of the converter that is demonstrated with an example.

In Chapter 3, the general operation of the active clamp snubber shown in Fig. 1.9 is explained in detail as are the modes of operation that a flyback converter with such a snubber goes through during a switching cycle. These modes of operation are analyzed and the results of the analysis are used to derive a procedure for the design of the converter that is demonstrated with an example.

In Chapter 4, experimental results obtained from converter prototypes of the two converters that have been designed according to the design procedure presented in Chapters 2 and 3 are presented and a comparison of the efficiency of flyback

converters with each of the two snubbers operating under various input voltage and output load conditions is made.

In Chapter 5, the contents of the thesis are summarized, the contributions and conclusions of this thesis are presented.

Chapter 2

2 Regenerative Snubber Circuits

2.1 Introduction

As was mentioned in Chapter 1, passive snubbers that do not dissipate energy but regenerate it are the most efficient passive snubbers. In this chapter, the operation of a flyback converter with a passive regenerative energy snubber is explained in detail. First the general operation of the converter is explained, then the converter's modes of operation are explained in greater detail. From the converter's modes of operation, equations that define key parameters are derived and these equations are then used to develop a procedure for the design of the converter. This design procedure is demonstrated with an example and the parameters determined by the procedure were used in the construction of a converter prototype that was used to obtain experimental results that will be presented in Chapter 4.

2.2 Converter Operation

The flyback converter with the regenerative energy snubber that is discussed in this thesis is shown in Fig. 2.1. The converter is a standard flyback converter with a passive snubber that consists of snubber capacitor C_{clamp}, diodes D_1 and D_{reg}, and an auxiliary winding N_t that is taken from the flyback transformer. An external inductor L_r can be connected in series with the auxiliary transformer winding if additional inductance is needed to limit the current through C_{clamp} and D_{reg}, as will be explained later in this section.

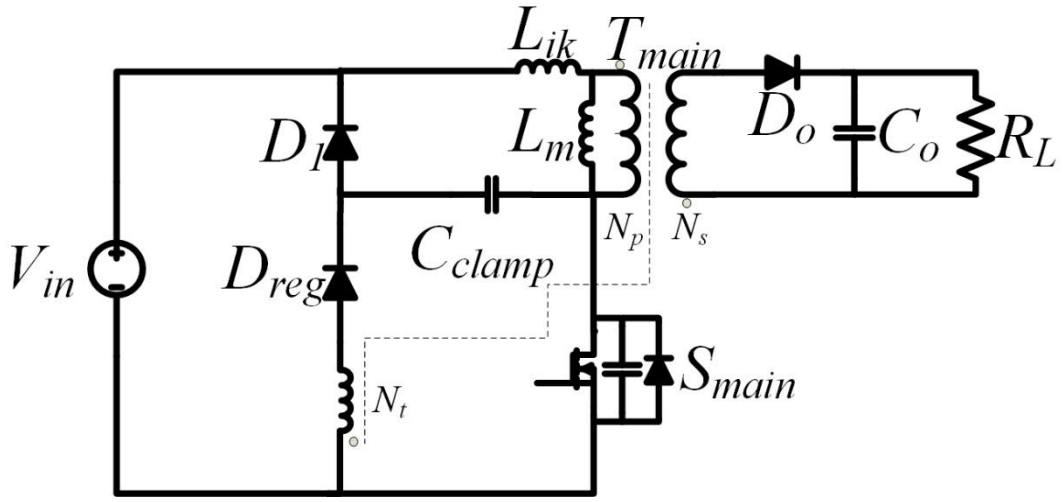

Fig. 2.1 A flyback converter with a regenerative snubber.

The snubber circuit that is shown in Fig. 2.1 consists of the snubber diodes D_1, D_{reg}, the clamp capacitor $C_{clamp.}$, and the extra winding that is coupled with the transformer.

The symbols in Fig. 2.1 are as follows:

S_{main} is the main switch, C_{clamp} is the clamp capacitor, T_{main} is the transformer, L_{ik} is the leakage inductance of the transformer, L_m is the magnetizing inductance of the transformer, N_p is the number of turns for the primary side of the transformer, N_s is the number of turns for the secondary side of the transformer, N_t is the number of turns for the territory winding of the transformer, D_1 and D_{reg} are the snubber diodes, V_{in} is the input voltage, V_o is the output voltage, C_o is the filter capacitor,D_{o1} is the output rectifier.

The transformer has the following turns ratio:

$$n_s = \frac{N_s}{N_p} \tag{2-1}$$

$$n_t = \frac{N_t}{N_p} \tag{2-2}$$

where N_p, N_s, and N_t are the number of turns of the primary, secondary, and territory windings respectively.

The magnetizing inductance of the transformer L_m is considered to be large compared with the leakage inductance.

2.2.1 General Converter Operation

The converter works as follows: when the main switch S_{main} is turned off, the transformer leakage inductance energy is transferred to the snubber capacitor C_{clamp} through the diode D_1. Eventually, the current through D_1 and C_{clamp} reduces to zero. When the switch is turned on at the beginning of the next switching cycle, C_{clamp} discharges through the switch, the diode D_{reg}, and the auxiliary winding. Since the auxiliary winding is coupled to the main transformer, energy from C_{clamp} is stored in the transformer. This energy is released to the output along with the energy that is normally stored in the flyback transformer when the switch is turned off.

2.2.2 Modes of Operation with analysis:

The converter has five time intervals in a switching cycle at the steady-state operation.

To simplify the steady-state analysis, the following assumptions are made:

- Switches and diodes are ideal.
- Inductors and capacitors are ideal without any parasitic elements.
- The capacitor C_o is large enough to keep the output voltage V_o constant.
- The non-ideal transformer is modeled by adding a leakage inductance and a magnetizing inductance to an ideal transformer.

Mode 1 ($t_o < t < t_1$)

This mode starts at t_o, when the current in the regenerative branch stops flowing. The current through L_{ik} and L_m increases linearly as shown in the equation (2-4). The snubber is completely idle in this mode. Moreover, there is no energy transfer from the primary to the secondary side. This mode is shown in Fig. 2.2.

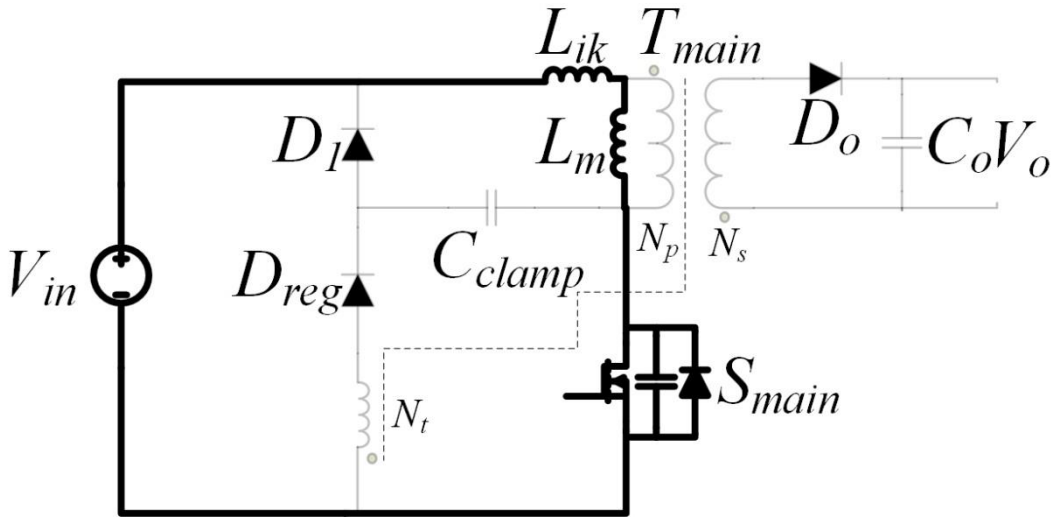

Fig. 2.2 Circuit diagram during the first mode.

Equation (2-3) represents the differential equation for this mode. The solution represents the current through the magnetizing inductance, which is shown in equation (2-4).

$$V_{in} = (\mathrm{L_m} + \mathrm{L_{ik}})\frac{\mathrm{di_{Lm}}}{\mathrm{dt}} \tag{2-3}$$

$$\mathrm{i_{lm}(t)} = \mathrm{i_{lik}(t)} = \frac{\mathrm{v_{in}}}{\mathrm{L_m} + \mathrm{L_{ik}}}\mathrm{t} + \mathrm{i_{L_m}(t_0)} \tag{2-4}$$

Mode 2 ($t_1 < t < t_2$)

This mode starts as soon as the switch is turned off at t_1. The energy from leakage inductance and magnetizing inductance will start releasing to C_{clamp} via D_1. The voltage across C_{clamp} and the current through both L_m and L_{ik} are shown in equations (2-7), (2-8) respectively. The time interval for this mode is very short. This mode ends when D_{o1} turns on at t_2. This mode is shown in Fig. 2.3.

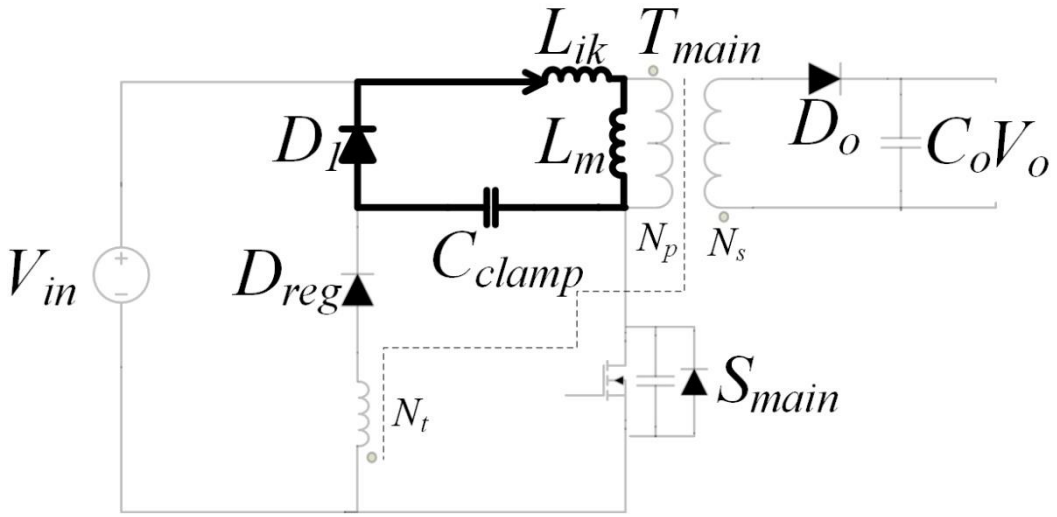

Fig. 2.3 Circuit diagram during the second mode.

Equations (2-5) and (2-6) represent the differential equations for this mode, and the solution gives the voltage across the clamp capacitor, and the current through the magnetizing inductance, which are shown in equations (2-7) and (2-8).

$$(\mathrm{L_m} + \mathrm{L_{ik}})\mathrm{C}\frac{\mathrm{d}^2\mathrm{v}_{c_{clamp}}(\mathrm{t})}{\mathrm{dt}^2} + v_{c_{clamp}}(\mathrm{t}) = 0 \tag{2-5}$$

$$\mathrm{i}_{\mathrm{L_m}}(\mathrm{t}) = \mathrm{i}_{\mathrm{L_{ik}}}(\mathrm{t}) = \mathrm{C}\frac{\mathrm{dv}_{c_{clamp}}(\mathrm{t})}{\mathrm{dt}} \tag{2-6}$$

$$V_{c_{clamp}}(t) = v_{c_{clamp}}(t_1)\cos(\omega_1 t) + i_{L_m}(t_1)\, Z_1 \sin(\omega_1 t) \tag{2-7}$$

$$i_{L_m}(t) = \frac{v_{c_{clamp}}(t_1)}{Z_1}\sin(\omega_1 t) + i_{L_m(t_1)}\cos(\omega_1\, t) \tag{2-8}$$

$$\omega_1 = \sqrt{\frac{1}{\mathrm{C}(\mathrm{L_{ik}} + \mathrm{L_m})}} \tag{2-9}$$

$$\mathrm{Z_1} = \sqrt{\frac{\mathrm{L_{ik}} + \mathrm{L_m}}{\mathrm{C}}} \tag{2-10}$$

where ω_1 is the angular frequency, and Z_1 is the characteristic impedance.

Mode 3 ($t_2 < t < t_3$)

This mode starts at t_2 when D_{o1} turns on. During this mode the energy from magnetizing inductance is transferred to the output via D_{o1}, and the energy from leakage inductance continues releasing to C_{clamp}. This mode ends at t_3 when the whole energy of the leakage inductance is transferred to C_{clamp}. The voltage across the C_{clamp}, and the current through L_{ik} are shown in equations (2-14) and (2-15). This mode is shown in Fig. 2.4.

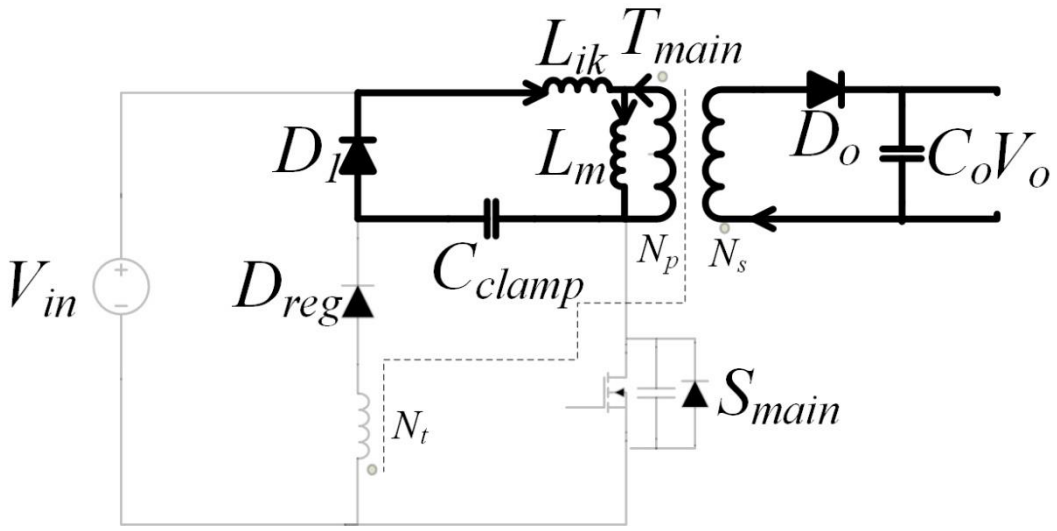

Fig. 2.4 Circuit diagram during Mode 3.

Equations (2-11), (2-12), and (2-13) represent the differential equations for this mode, and the solution gives the voltage across the clamp capacitor as well as the current through the leakage inductance, which are shown in equations (2-14) and (2-15).

$$v_{c_{clamp}}(\mathrm{t}) + \mathrm{L_{ik}}\frac{\mathrm{di_{L_{ik}}(t)}}{\mathrm{dt}} - \mathrm{v_o}\frac{\mathrm{N_p}}{\mathrm{N_s}} = 0 \tag{2-11}$$

$$\mathrm{i_c(t)} = \mathrm{C}_{clamp}\frac{dv_{c_{clamp}}(\mathrm{t})}{\mathrm{dt}} \tag{2-12}$$

$$v_{c_{clamp}}(\mathrm{t}) + \mathrm{l_{ik}}\,\mathrm{C}_{clamp}\,\frac{\mathrm{d}^2 v_{c_{clamp}}}{\mathrm{dt}^2} - \mathrm{v_o}\frac{\mathrm{N_p}}{\mathrm{N_s}} = 0 \tag{2-13}$$

$$v_{c_{clamp}}(t) = \left(v_{c_{clamp}}(t_2) - v_o\frac{N_p}{N_s}\right)\cos(\omega_2 t) + i_{L_{ik}}(t_2)Z_2\sin(\omega_2 t) - v_o\frac{N_p}{N_s} \tag{2-14}$$

$$i_{L_{ik}}(t) = \frac{v_{c_{clamp}}(t_2) - v_o\frac{N_p}{N_s}}{Z_2}\sin(\omega_2 t) + i_{L_{ik}}(t_2)\cos(\omega_2 t) \tag{2-15}$$

where:

$$\omega_2 = \sqrt{\frac{1}{C_{clamp} L_{ik}}} \tag{2-16}$$

$$Z_2 = \sqrt{\frac{L_{ik}}{C_{clamp}}} \tag{2-17}$$

where ω_2 is the angular frequency, and Z_2 is the characteristic impedance.

Mode 4 ($t_3 < t < t_4$)

This mode starts at t_3 when the current through the leakage inductance stops flowing. The energy from the magnetizing inductance is still transferred to the output. This mode ends at t_4 when the switch is turned on. The current through L_m is shown in the equation (2-19). This mode is shown in Fig. 2.5.

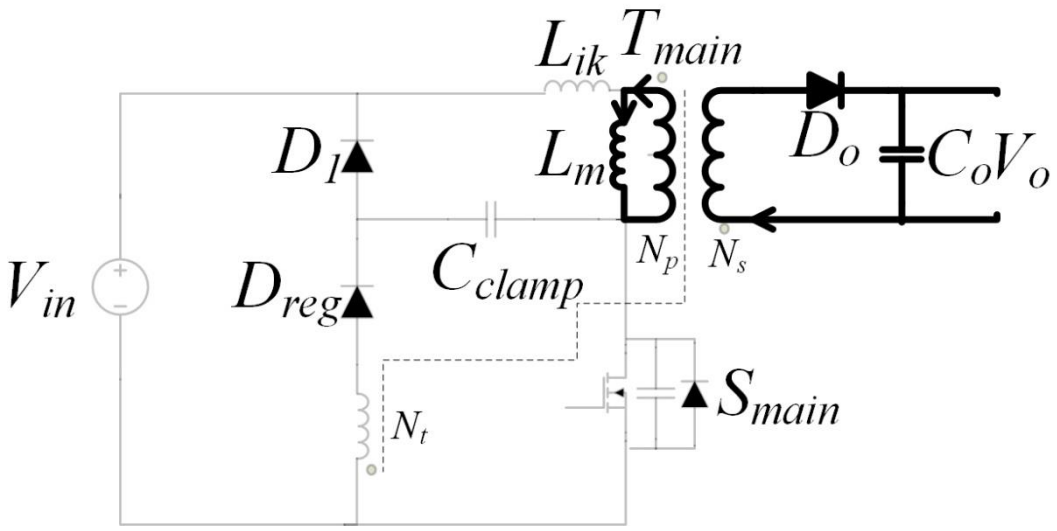

Fig. 2.5 Circuit diagram during Mode 4.

Equation (2-18) represents the differential equations for this mode, and the solution gives the current through magnetizing inductance, which is shown in equation (2-19).

$$L_m \frac{di_{L_m}}{dt} = v_o \frac{N_p}{N_s} \tag{2-18}$$

$$i_{L_m}(t) = \frac{1}{L_m} v_o \frac{N_p}{N_s} t + i_{L_m}(t_3) \tag{2-19}$$

Mode 5 ($t_4 < t < t_5$)

This mode starts at t_4 when turning on the switch. The energy from magnetizing inductance stops releasing to the output. The energy in C_{clamp} starts discharging through the switch, D_{reg}, and the territory winding. Moreover, the current increases linearly through L_{ik} and L_m. The voltage across C_{clamp} and the current through territory winding are shown in equations (2-22) and (2-23). This mode ends at t_5 when the current through the territory winding decreases to zero. This mode is shown in Fig. 2.6.

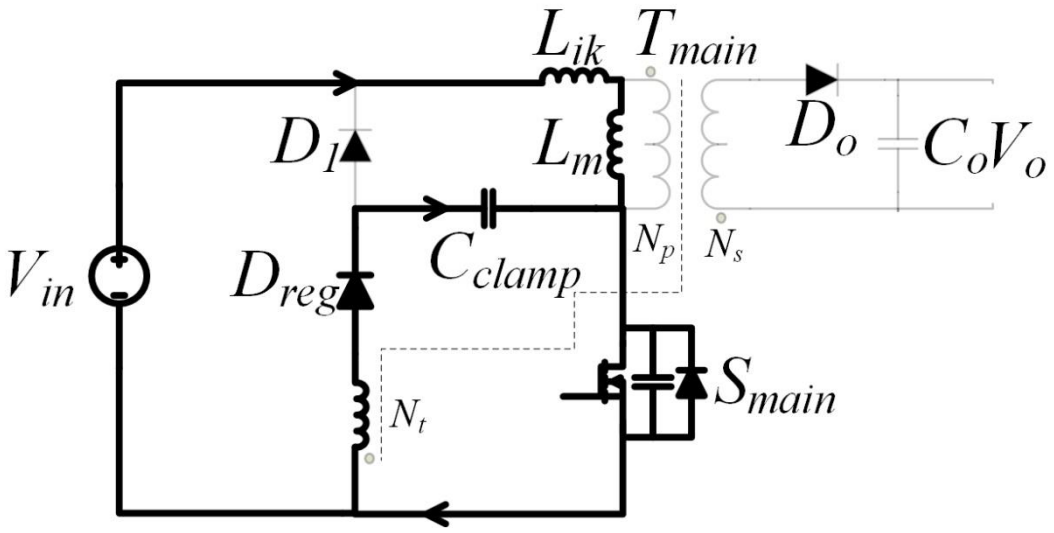

Fig. 2.6 Circuit diagram during Mode 5.

Equations (2-20) and (2-21) represent the differential equations for this mode, and their solution gives the voltage across clamp capacitor and the current through the clamp capacitor, which are shown in equations (2-22) and (2-23).

$$L_{ik}\, n_t^{\,2}\, C\, \frac{d^2 v_{c_{clamp}}(t)}{dt^2} + n_t v_{in} - v_{c_{clamp}}(t) = 0 \tag{2-20}$$

$$i_c(t) = C\frac{dv_{c_{clamp}}}{dt} \tag{2-21}$$

$$v_{c_{clamp}}(t) = v_{c_{clamp}}(t_4)\, cos(\omega_3 t) + n_t Z_3 i_c(t_4)\, sin(\omega_3 t) \tag{2-22}$$

$$i_c(t) = \frac{-v_0(t_4)}{n_t Z_3}\sin(\omega_3 t) + i_c(t_4)\cos(\omega_3\, t) \tag{2-23}$$

where:

$$\omega_3 = \sqrt{\frac{1}{C_{clamp} L_{ik}}} \tag{2-24}$$

$$Z_3 = \sqrt{\frac{L_{ik}}{C_{clamp}}} \tag{2-25}$$

where ω_3 is the angular frequency, and Z_3 is the characteristic impedance.

2-3 Design procedure

The equations for the modes of operation that were shown in the previous section can be used to generate graphs of steady-state characteristics for this converter.

A program can be implemented by a computer program such as C or MATLB. In the steady-state , the current and voltage of any converter component at the start of a switching cycle must be the same as that at the end of the switching cycle. If the equations presented in the previous section are used by a program to track component current and voltage values throughout a switching cycle when the converter is operating with a given set of component values, then the program can determine if the converter is operating in the steady-state. Once this has been determined , then the appropriate steady-state component voltage and current values can be found. If this is done for a number of component value sets, then characteristic curves and graphs can be generated.

The characteristic graphs that are generated and shown illustrate the effects that changing a particular component value can have on converter voltages and currents. With these graphs, it is possible to systematically design a converter that would allow appropriate converter component values to be selected.

The minimum input voltage for the designed converter is 36 Volts ($V_{in,min}$), and the maximum input voltage is 72 Volts ($V_{in,max}$). The output voltage is always 12 Volts (V_o). The maximum output power is 100 Watts. There are many parameters for the converter. Some of these parameters will be assumed, and others will be derived or chosen according to design curves.

In this section, several guidelines that should be considered in the design of the flyback converter with the regenerative energy snubber shown in Fig. 2.1 are discussed. It should be noted that any design procedure that takes into account the following design considerations is iterative and thus several iterations are required before an appropriate design is selected.

1) Select the value of maximum duty cycle

While a flyback converter has the ability to work at a duty cycle higher than 50%, the maximum duty cycle will be chosen at 50%. As the duty cycle increases, the peak primary current decreases, but the peak secondary current and voltage stress on the switch both increase. Thus, it is a good compromise to choose D_{max}=50%.

2) Select magnetizing inductance for Flyback transformer:

Adding a regenerative snubber circuit does not considerably change the primary current waveforms from the one seen in the regular Flyback converter; therefore, the common method for determining the magnetizing inductance can be used. Magnetizing inductance can be chosen according to several considerations. For example, it can be chosen in order to ensure continuous conduction mode CCM, or it can be chosen to maintain a maximum ripple in the current at the primary or secondary value. In this design, CCM will be used. The maximum allowed ripple for 1 amp. The magnetizing inductance can be calculated using the following equation, which represents the rate of change of a current through an inductor:

$$\frac{\Delta \, I_{L_M}}{\Delta \, t} = \frac{V_{in,min} - V_{R_{dc,on}}}{L_m} \tag{2-26}$$

where $\Delta \, I_{L_m}$ is the ripple current in the primary, $V_{R_{dc,on}}$ is the voltage drop across the switch when the switch is in on-state and its value is around 1 Volt.

By using the following values: $\Delta \, I_{L_m} = 1$ amp;

$\sec \Delta \, t = \frac{1}{f_{sw}} * D_{max} = \frac{1}{50000} * .5 = 1 * 10^{-5}$

where f_{sw} is the switching frequency, and D_{max} is the maximum duty cycle, then L_m can be calculated and it was found to be L_m=0.35 mH.

3) Choosing transformer turns ratio

Transformer turns ratio also affects the voltage stress on the main switch as duty cycle does. Transformer turns ratio and duty cycle are related to each other. If a small maximum duty cycle is chosen, then the transformer turns ratio should be high and vice versa. Since the maximum duty cycle was chosen to be 50% in this design, determining turns ratio will not be hard. It can be calculated by using the following equation, which represents the conversion ratio for the flyback converter:

$$\frac{1}{n_s} = \frac{V_{in,min} - V_{R_{dc,on}}}{V_o + \mathrm{V_{fw}}} * \frac{\mathrm{D_{max}}}{1 - \mathrm{D_{max}}} \qquad (2\text{-}27)$$

where V_{fw} is the voltage drop across the output rectifier during forward biased, which is around 0.8 Volts. By substituting the known values in the above equation, it can be found that n_s=0.366. Hence, if 80 turns were chosen for the primary, then almost 30 turns will be used for the secondary.

4) Selecting leakage inductance

As mentioned previously, leakage inductance is an undesirable meaning it is desirable to keep it as low as possible. It is usually less than 10% of magnetizing inductance. In this design, the measured leakage inductance is 10 µH.

5) Select the value of turns ratio territory to primary (n_t)

Choosing the values of n_t and clamp capacitor C_{clamp} are the most important components in designing the converter as they affect the efficiency of the converter. The design curves approach will be used to determine the proper values for these parameters. In this section the design procedure for choosing n_t will be illustrated, and in the following section the design procedure for choosing the C_{clamp} will be illustrated. Fig. 2.7 shows the design curves.

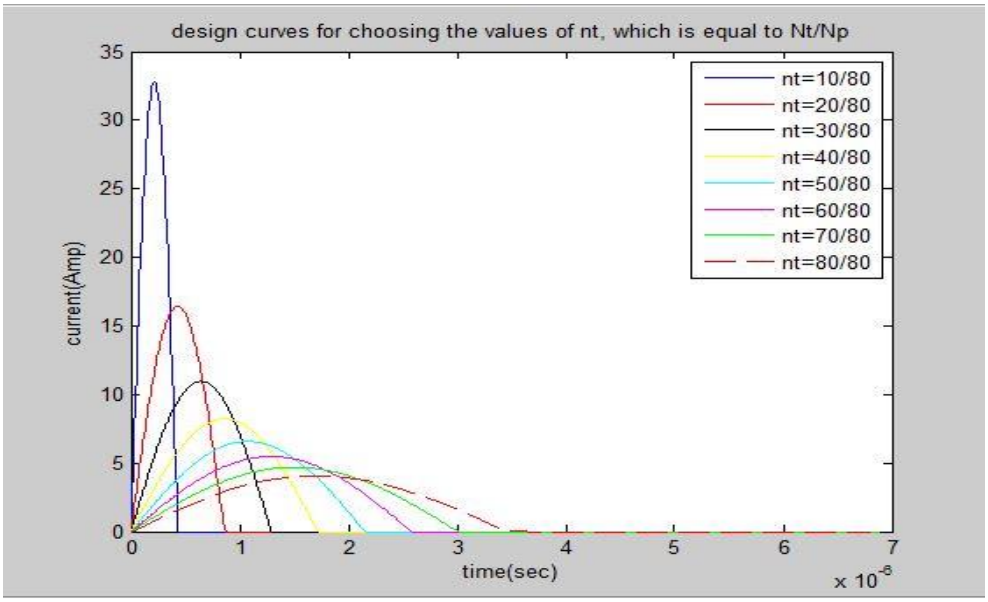

Fig. 2.7 Design curves for choosing n_t

The horizontal axes represents the on-time for the main switch while the vertical axes represents the current through the coupled winding and the clamp capacitor. As can be seen from Fig. 2.7, the value of n_t determines how much time is required to discharge the clamp capacitor. If the value of n_t is chosen to be small, it will result in high peak current, and this current will be added to the current in the main switch. Increasing the peak value of the current through the main switch is not a good choice. Thus, setting values of n_t to less than 1/4 should be avoided. On the other hand, as the value of n_t increases, the time required to discharge the clamp capacitor will be longer. For better performance, the time for discharging the clamp capacitor should be less than 25% of on-time for the switch [10]. Therefore, setting n_t values to more than 5/8 should be avoided. Thus, a good compromise value of n_t is = 0.5.

6) Select clamp capacitor C_{clamp}

Design curves will be used to select a proper clamp capacitor. The value of the clamp capacitor is even more critical than n_t. It affects the current through the output rectifier.

Fig. 2.8 shows the voltage across the clamp capacitor, and Fig. 2.9 shows the output rectifier current. As can be seen from Fig. 2.8, the clamp capacitor charges quickly with a higher maximum voltage when it has a small value. However, as the clamp capacitor increases in value, the time of the charge will be longer, and will yield a smaller maximum voltage. The time to charge the clamp capacitor should not be too

long. It should be less than 25% of the off-time for the switch [10]. Hence, the clamp capacitor should be between 100 nF and 175 nF.

Fig. 2.9 shows the current through the output rectifier with different clamp capacitor values. It is noticeable that as clamp capacitor values get smaller, the current through the output rectifier rises to its maximum value sharply. This results in a loss of ZCS turning on for the output rectifier. Therefore, setting clamp capacitor values to less than 100 nF should be avoided. A good compromise is to choose 150 nF as the clamp capacitor value because it provides ZCS turning on for the output rectifier and charges in less than 25% of the off-time for the switch.

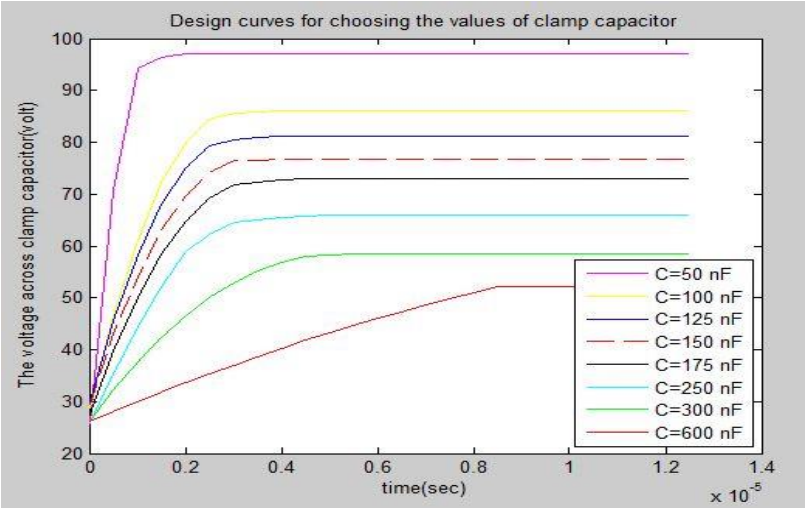

Fig. 2.8 Voltage across clamp capacitor

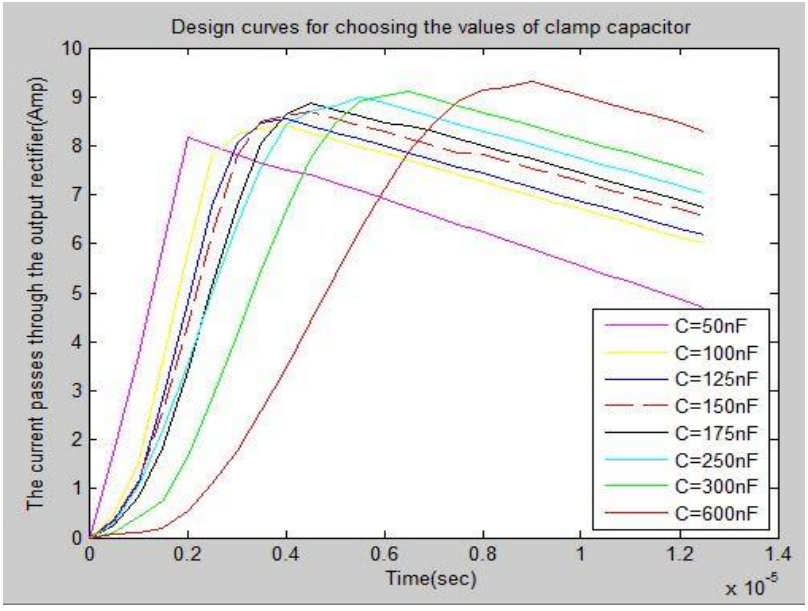

Fig. 2.9 Current through output rectifier

7) Selecting D_1

D_1 should be selected to be able to carry maximum current that occurs during the worst scenario, which happens at both the minimum input voltage and full load. It should also be chosen with a voltage rating higher than the maximum reverse voltage.

The peak current through D_1 is equal to the maximum current in the magnetizing inductance $I_{L_{m,max}}$.

The maximum current through D_1 is equal to the maximum current through the magnetizing inductance. The magnetizing inductance current can be approximated using the following equation:

$$I_{L_{m,pk}} = I_{L_{m,avg}} + \Delta I_{L_M} \approx \frac{n_s \, . V_o}{(1 - D_{\max}) . R_L} + \Delta I_{L_M} \qquad (2\text{-}28)$$

By using $n_s = 0.37, V_o = 12v, D_{max}, R_L = 1.5, \Delta I_{L_M} = 1\ A$, it can be found that $I_{L_{m,pk}}$ is equal to 6.92A.

Equation (2-26) can be used to determine the maximum current in the worst case scenario. By knowing the maximum values, the rating of current and voltage for D_1 can be calculated by taking into account a safety margin as follows: Current rating = safety factor *maximum current. The maximum reverse voltage applied across D_1 can be approximately determined by the following equation (2-29) [10]:

$$v_{D1,max} \approx 2 * I_{Lm_{max}} * \sqrt{\frac{L_{ik}}{C_{clamp}}} - \frac{V_o}{n_s} \qquad (2\text{-}29)$$

By using $I_{Lm_{max}} 6.92A,\ n_s = 0.37, V_o = 12\ v, L_{ik} = 10\ uH, C_{clamp} = 150\ nF$ it can be found that $v_{D1,max} = 80.5v$.

Equation (2-27) shows the approximated value for the maximum reverse voltage across D_1 in the worst case scenario.

The maximum reverse voltage rating should also be higher than the voltage calculated in equation (2-29). A safety margin is necessary to ensure that the device does not burn if the voltage or current increases slightly above the maximum value for any reason.

8) Select the switch

The switch, which is a MOSFET, is chosen based on maximum stress voltage, maximum peak current, total power losses, maximum allowed operating temperature, and current driver capability. Different transistors have different $R_{ds,on}$, which determines conduction losses, thus, it is better to minimize $R_{ds,on}$ but transistors with low $R_{ds,on}$ are more expensive. Therefore, there should be a compromise between the cost and the value of $R_{ds,on.}$

Maximum current passes through the switch can be approximated as shown in equation (2-30):

$$\boldsymbol{I_{ds,max}} \approx \frac{\boldsymbol{P_o}}{\eta\, v_{in,min}\, D_{max}} + I_{Cclamp,peak,mode\,5} \qquad (2\text{-}30)$$

By using P_o=100, η =80%, $V_{in,min}$ =36V, D_{max} =0.5, $I_{Cclamp,peak,mode\,5}$ =9.72A, it can be found that $\boldsymbol{I_{ds,max}} \approx$ 16.6A.

Equation (2-30) shows that the current through the main switch is composed of two components. The first component represents the average input current during the on-time of the main switch. This component is supplied directly from the input source. The second component, on the other hand, represents the current through the switch supplied from the snubber circuit. The second component causes a hump in the waveform of the current through the main switch.

The maximum voltage stress across the switch can approximately be calculated from equation (2-31) [x]. Equation (2-31) shows that the maximum voltage stress is equal to the sum of input voltage, reflected voltage from the output, and some extra voltage due to resonant between the leakage inductance and the clamp capacitor.

$$v_{ds,peak} \approx v_{in,max} + \frac{v_o}{n_s} + \sqrt{\frac{L_{ik}}{c_{clamp}}}\; I_{Lm_{max}} \qquad (2\text{-}31)$$

By using $V_{in,max}$=72V, V_o=12V, n_s=0.366, L_{ik}=10 µH, Cclamp=150nF, it can be found that =160.9V.

A safety margin should be considered when choosing the ratings of the switch.

9) Selecting D_{reg}

D_{reg} should be selected to be able to carry the maximum current that occurs during the worst case scenario, which happens at both the minimum input voltage and full load. It should also be chosen with a voltage rating higher than the maximum reverse voltage. The current through D_{reg} is equal to the current in the clamp capacitor in Mode 5, and the maximum value will be equal to 9.72A.

A diode with a forward current rating higher than the maximum current by a safety margin factor should be chosen.

The voltage stress across the D_{reg} can be approximated using the following equation (2-32):

$$v_{D_{reg,max}} = v_{ds,peak} - \frac{V_o}{n_s} \tag{3-32}$$

By using $v_{ds,peak=}160.8\ v, V_o = 12\ v,\ n_s = 0.37,$ it can be found that $v_{D_{reg,max}} = 127.6\ v$

10) Select output rectifier:

Adding the regenerative snubber does not alter significantly the maximum voltage stress across the output diode. The average current through the output rectifier is equal to the load current.

The maximum reverse voltage across the output rectifier can be simply calculated by using equation (2-33):

$$v_{D1,max} = \mathrm{v_o} + \mathrm{v_{in,max} n_s} \tag{2-33}$$

The maximum forward current through the output rectifier can be approximately calculated by using equation (2-34).

$$\mathrm{I_{D1,max}} \cong \frac{2\mathrm{P_o}}{\mathrm{v_o}(1 - \mathrm{D_{max}})} \tag{2-34}$$

By using $\mathrm{v_{in,max}} = 72\mathrm{v}$, $\mathrm{ns} = 0.37$, $\mathrm{v_o} = 12\mathrm{v}$, it can be found that $\mathrm{v_{D1,max}} = 38.64\mathrm{v}$. By using $P_o = 100w$, it can be found that $\mathrm{I_{D_{1,max}}}$ is equal to 33.33 Amp

A safety margin should always be considered when choosing the ratings of the switch.

11) Select output capacitor:

In the flyback topology, there is no output inductor filter and this means that the size of the output capacitor should be bigger than other topologies, e.g., forward converters. The output capacitor has to be selected in order to meet the following four parameters: capacitance, ESR (equivalent series resistance), RMS current rating and voltage rating. Choosing a capacitor with a desired value and a required voltage rating gives a ripple current rating lower than required. There are two solutions to meet the current ripple requirement: either increasing the voltage rating or connecting several capacitors on parallel. Choosing the output capacitor can be facilitated by the following equation:

$$\Delta V = \frac{I * \Delta t}{C} \qquad (2\text{-}35)$$

If it is assumed that a 200uF capacitor is being discharged by a 20 Amp load current over 1 usec, then ΔV will be equal to 0.1 Volts. If the peak to peak ripple current is 5 Amps and the ESR of this capacitor is 0.145 Ohms, then the voltage ripple can be calculated to be $\Delta V = \Delta I * ESR = 5 * 0.145 = 0.725$ Volts

If 0.725 volts is higher than the allowed ripple voltage, the capacitors need to be connected in parallel. If two capacitors are connected in parallel, the equivalent ESR for both of them is $\frac{0.145*0.145}{0.145+0.145} = 0.0725\ Ohms$, and $\Delta V = 5 * 0.0725 = 0.3625$ Volts . Assuming that the maximum allowed voltage ripple is 0.4 Volts, then connecting two capacitors on parallel satisfies the requirements.

Fig. 2.10 shows the designed flyback converter with the energy regenerative snubber.

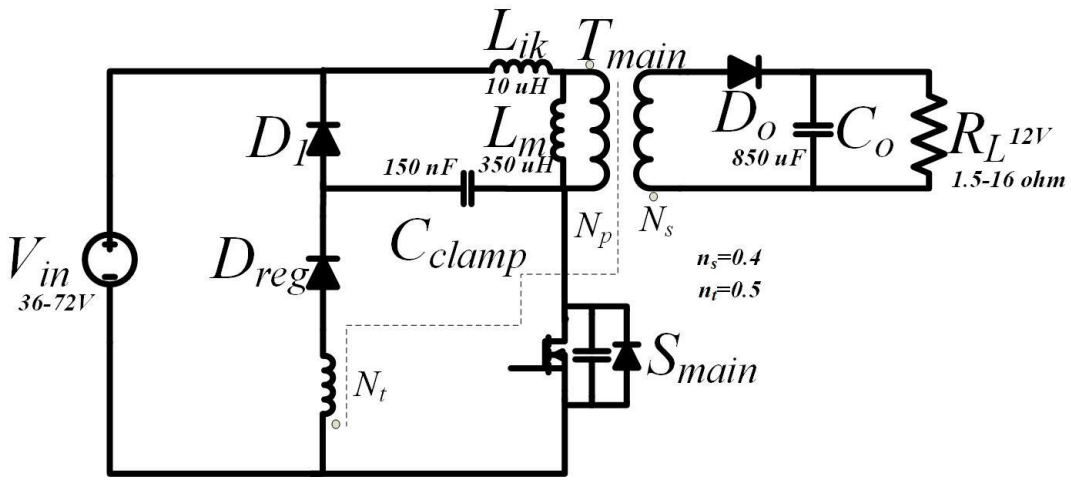

Fig. 2.10 The designed flyback converter with energy regenerative snubber.

Current and voltage ratings for MOSFET and diodes will be mentioned in Chapter 4 with full experimental results.

2.4 Conclusion

In this chapter, the operation, analysis, and design of a flyback converter with a passive regenerative energy snubber were presented. The general operation and the converter's modes of operation were explained, equations that define the operation of the converter for each operation mode were derived, and these equations were used to develop a procedure for the design of the converter. Based on the analysis and design, the following characteristics were identified:

- When n_t is very small, then the switch suffers from high peak current.
- If C_{clamp} is very small, then the current in the output rectifier rises very quickly.

The design procedure was demonstrated with an example for the design of a converter with input voltage V_{in} = 36-72 V, output voltage V_o = 12 V, maximum output power $P_{o.max}$ = 100 W, and switching frequency f_{sw} = 50 kHz. Based on the design example, the values of certain key converter parameters were obtained and these parameter values were used to build a converter prototype, used to obtain the experimental results that will be described in Chapter 4.

Chapter 3

3 Active clamp technique for Flyback converter

3.1 Introduction

As was mentioned in Chapter 1, active clamp snubbers are the most popular type of active snubbers in flyback converters because of their simplicity, low cost, and high efficiency. In this chapter, the operation of a flyback converter with an active clamp snubber is explained in detail. First the general operation of the converter is explained, then the converter's specific modes of operation are explained. From the converter's modes of operation, equations that define key parameters are derived and these equations are then used to develop a procedure for the design of the converter. This design procedure is demonstrated using an example, and the parameters determined by the procedure were used in the construction of a converter prototype, used to obtain experimental results that will be presented in Chapter 4.

3.2 Converter operation

The active clamp flyback converter discussed in this thesis is shown in Fig. 3.1. The converter has an active clamp that consists of switch S_{aux} and capacitor C_{clamp}, in addition to the typical elements found in all flyback converters including a transformer, a main switch (S_{main}), a secondary diode (D_{o1}) and an output filter capacitor (C_o). An external inductor L_r can be connected in series with the primary winding of the transformer if its leakage inductance is too small to help the main switch turn on with zero-voltage switching (ZVS).

The circuit diagram for a flyback converter with active clamp circuit is shown in Fig. 3.1.

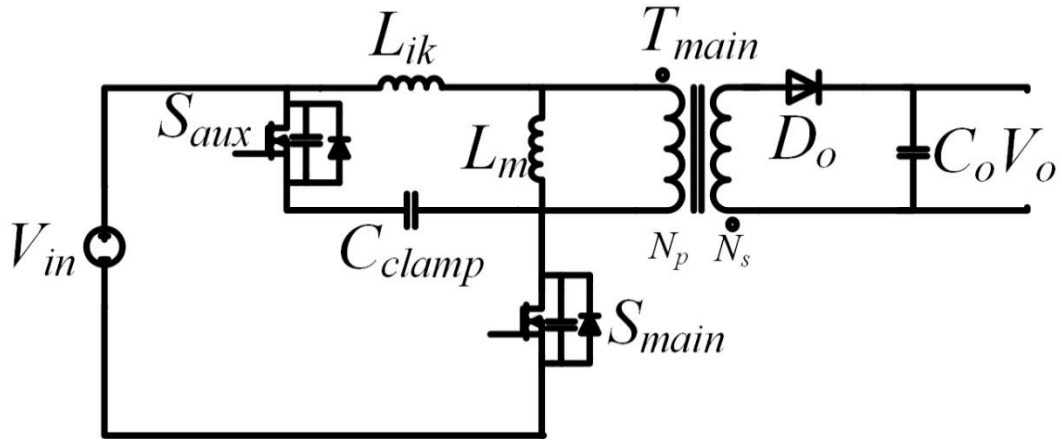

Fig. 3.1 Flyback converter with active clamp

The clamp circuit consists of the auxiliary switch (S_{aux}), and the clamp capacitor(C_{clamp}). If the leakage inductor is small and is not sufficient to produce the zero voltage transition, an external inductor L_r can be connected on series with the transformer in order to get the active clamp circuit working properly.

As can be seen in Fig. 3.1., there is a capacitor on parallel with each switch, and these capacitors are called output capacitors. Their values are much smaller than the value of the clamp capacitor. These capacitors will be charged and discharged through the operation of the flyback converter, which will be discussed during the survey of the modes of operation. The symbol C_r is equal to the parallel combination of the output capacitances of both switches. In order to achieve ZVS, the resonant period between the clamp capacitor and the leakage inductance must be greater than the turn off time of the main switch.

The symbols in Fig. 3.1 are as follows:

S_{main} is the main switch, S_{aux} is the auxiliary switch, C_{clamp} is the clamp capacitor, T_{main} is the transformer, and N_p is the number of turns for the primary side of the transformer. N_s is the number of turns for the secondary side of the transformer, V_{in} is the input voltage, V_o is the output voltage, and C_o is the filter capacitor. D_o is the output rectifier. L_{ik} is the leakage inductance of the transformer. L_m is the magnetizing inductance of the transformer. The transformer has the following turns ratio:

$$n_s = \frac{N_s}{N_p} \qquad (3\text{-}1)$$

where N_s and N_p are the number of turns for primary and secondary respectively.

3.2.1 General Converter Operation

The converter works as follows: when the main switch S_{main} is turned off, transformer leakage inductance energy is transferred to the snubber capacitor C_{clamp} through the body diode of S_{aux}. While current is flowing through its body diode, S_{aux} can be turned on with ZVS. After the current stops flowing through the C_{clamp}, it reverses direction and starts to flow "up" the transformer. When the main switch is about to be turned on to start the next switching cycle, S_{aux} is turned off and current starts to flow through the body diode of S_{main}, thus allowing it to turn on with ZVS. Eventually, the current in the transformer reverses direction and flows in the switch itself.

3.2.2 Modes of operations with analysis:-

In order to facilitate the operation of the converter the following assumptions are made:

1- The capacitors, diodes, and inductors are considered ideal; they do not have parasitic elements.

2- The switches are represented by adding the body diodes and the output capacitors because they are basic parts in the operation of the active clamp.

During a switching cycle, the converter enters a sequence of eight topological stages. What follows is a detailed description of the modes of operation.

Mode 1 ($t_0 < t < t_1$):

During this mode the main switch is on and the auxiliary switch is off. There is no current flowing in the snubber circuit. Energy is being stored in the main power transformer. Fig. 3.2 shows the flyback circuit during Mode 1. Equation (3-2) represents the differential equation for this mode, and equation (3-3) represents the solution of equation (3-2), which gives the current through the magnetizing inductance or the leakage inductance.

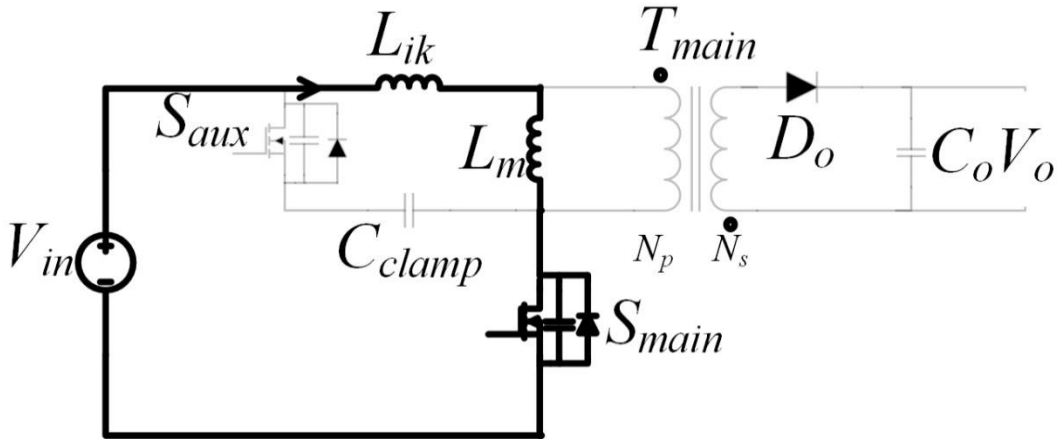

Fig. 3.2 Mode 1 ($t_0<t<t_1$)

$$v_{in} = (L_m + l_{ik})\frac{di_{Lm}}{dt} \tag{3-2}$$

$$i_{L_m}(t) = \frac{v_{in}}{L_m + L_{ik}}\,(t - t_o) + i_{L_m}(t_0) \tag{3-3}$$

Mode 2 ($t_1 < t < t_2$):

This mode starts when the main switch is turned off. The output capacitor of the main switch starts to charge, while the output capacitor of the auxiliary switch starts to discharge. Since the output capacitors for the switches are very small, this mode is brief. Fig. 3.3 illustrates the flyback circuit during Mode 2. Equations (3-4) and (3-5) represent the differential equations for this mode, and the solution is given in equations (3-6) and (3-7). (3-6) represents the voltage across the output capacitance of the switches, and (3-7) gives the current through the leakage inductance.

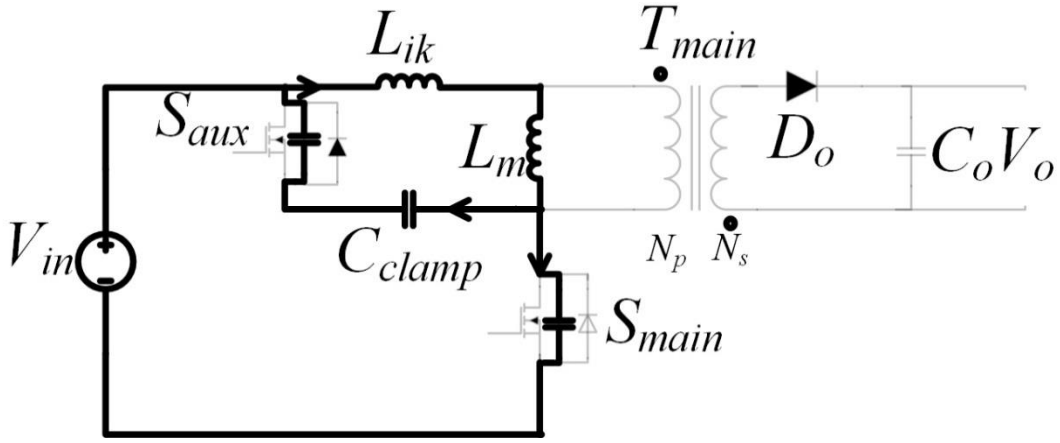

Fig. 3.3 Mode 2 ($t_1<t<t_2$)

$$\frac{d^2 v_{Cr}}{dt^2} C_r(L_{ik} + L_m) + v_{Cr}(t_1) = v_{in} \tag{3-4}$$

$$i_{c_r} = c_r \frac{dv_{c_r}(t)}{dt} \tag{3-5}$$

$$v_{Cr}(t) = v_{in}(1 - \cos(\omega_1 t)) + i_{L_{ik}}(t_1)\, Z_1 \sin(\omega_1 t) \tag{3-6}$$

$$i_{L_{ik}}(t) = \frac{v_{in}}{Z_1}\sin(\omega_1 t) + i_{L_{ik}}(t_1)\cos(\omega_1 t) \tag{3-7}$$

where

$$Z_1 = \sqrt{\frac{L_{ik} + L_m}{c_r}} \tag{3-8}$$

$$\omega_1 = \frac{1}{\sqrt{c_r(L_m + L_{ik})}} \tag{3-9}$$

Mode 3 ($t_2 < t < t_3$):

At time t_2, the output capacitor of the auxiliary switch is fully discharged, and its body diode starts to conduct. On the other hand, the output capacitor for the main switch is fully charged during this mode, and the main switch stops conducting completely. Fig. 3.4 illustrates the flyback circuit during Mode 3. The differential equations for this mode are given in equations (3-10) and (3-11), and the solutions are given in equations (3-12), and (3-13). (3-12) shows the voltage across the clamp capacitor, and (3-13) shows the current through the leakage inductance.

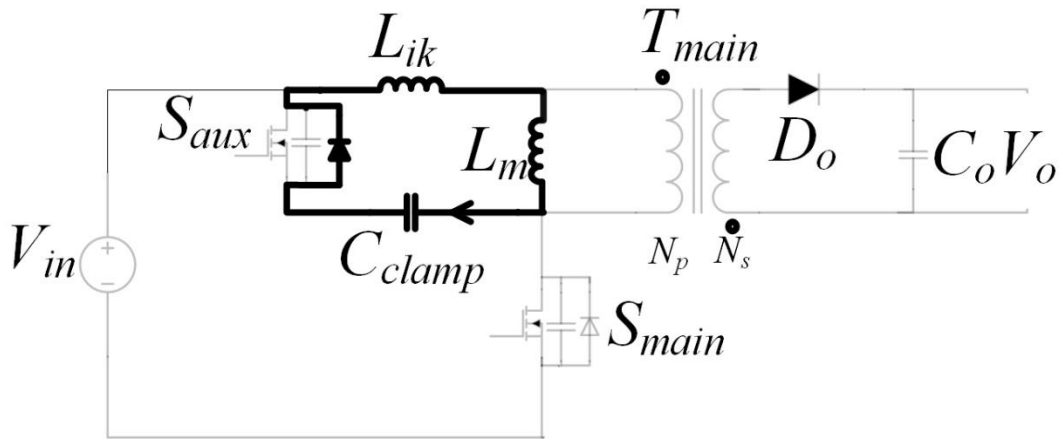

Fig. 3.4 Mode 3 ($t_2<t<t_3$)

$$L_{ik}\, C_{clamp} \frac{d^2 v_{c_{clamp}}}{dt^2} + n\, v_o + v_{c_{clamp}}(t) = 0 \tag{3-10}$$

$$i_{L_{ik}}(t) = c_{clamp} \frac{dv_{c_{clamp}}(t)}{dt} \tag{3-11}$$

$$v_{clamp}(t) = n\, v_o \cos(\omega_2 t) + i_{L_{ik}}(t_2)\, Z_2 \sin(\omega_2 t) \tag{3-12}$$

$$i_{L_{ik}}(t) = i_{L_{ik}}(t_2)\cos(\omega_2 t) - \frac{n\, v_o}{Z_2}\sin(\omega_2 t) \tag{3-13}$$

$$Z_2 = \sqrt{\frac{L_{ik} + L_m}{c_{clamp}}} \tag{3-14}$$

$$\omega_2 = \frac{1}{\sqrt{c_{clamp}(L_m + L_{ik})}} \tag{3-15}$$

Mode 4 ($t_3 < t < t_4$):

At time t_3, the primary voltage of the main transformer becomes equal to $-n_s V_0$; consequently, the secondary diode starts to conduct. During this mode or the previous one, the auxiliary switch can be turned on with ZVS. This mode ends when the snubber capacitor current reaches zero. Fig. 3.5 illustrates the flyback circuit during Mode 4. Solving the differential equations (3-16) and (3-17) gives the current through leakage inductance, and the voltage across the clamp capacitor, as shown in equations (3-18), and (3-19) .

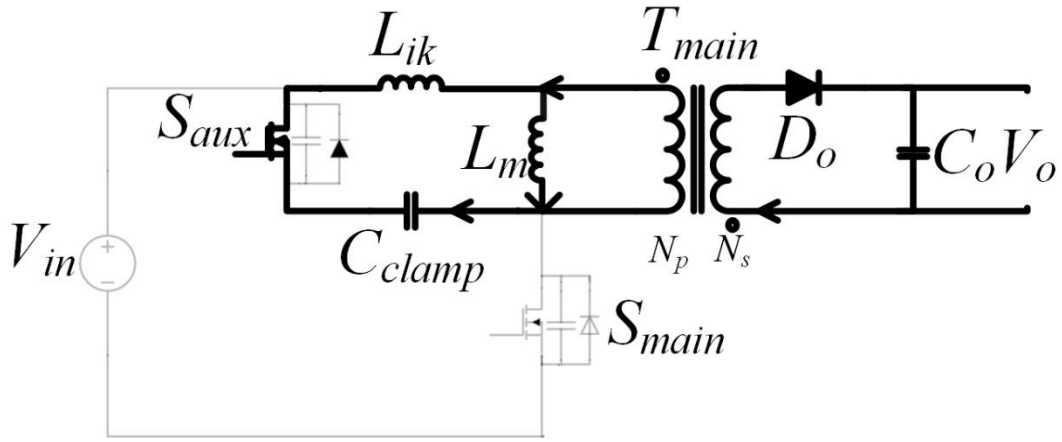

Fig. 3.5 Mode 4 ($t_3<t<t_4$)

$$i_{L_m}(t) = i_{L_m}(t_3) - \frac{n\, v_o}{L_m}\, t \tag{3-16}$$

$$L_{ik}\, C_{clamp}\, \frac{d^2 v_{c_{clamp}}(t)}{dt^2} + v_{clamp}(t) = n\, v_o \tag{3-17}$$

$$i_{L_{ik}}(t) = \frac{n * v_o - v_{clamp}(t)}{Z_3}\sin(\omega_3 t) + i_{L_{ik}}(t_3)\cos(\omega_3\, t) \tag{3-18}$$

$$v_{clamp}(t) = n\, v_o - \left(n\, v_o - v_{clamp}(t_3)\right)\cos(\omega_3\, t) + i_{L_{ik}}(t_3)\, Z_3\, \sin(\omega_3 t) \tag{3-19}$$

$$Z_3 = \sqrt{\frac{L_{ik}}{c_{clamp}}} \tag{3-20}$$

$$\omega_3 = \frac{1}{\sqrt{c_{clamp}.(L_{ik})}} \quad (3\text{-}21)$$

Mode 5 ($t_4 < t < t_5$):

This mode is the same as Mode 4 but the snubber capacitor current flows in the reverse direction. Fig. 3.6 shows the flyback circuit during Mode 5.

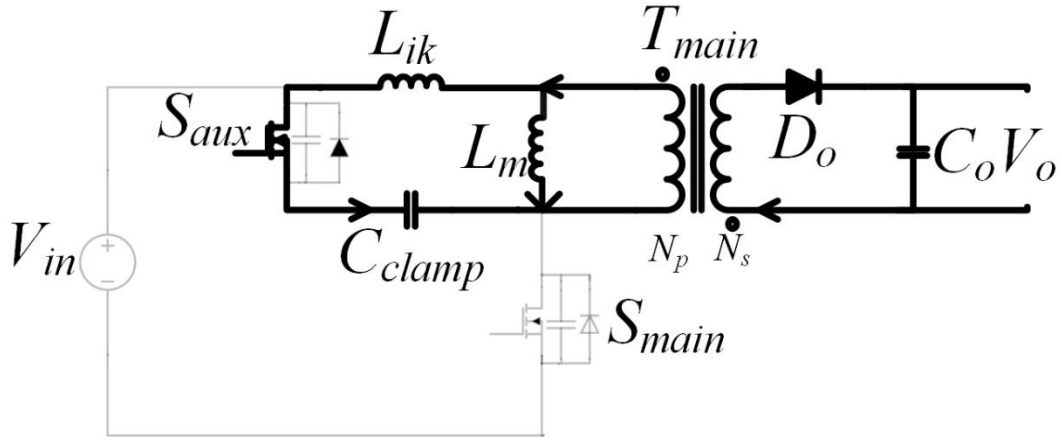

Fig. 3.6 Mode 5 ($t_4<t<t_5$)

Mode 6($t_5 < t < t_6$):

At t_5 the auxiliary switch is turned off. The output capacitor of the main switch starts to discharge, while the output capacitor of the auxiliary switch starts to charge. Fig. 3.7 illustrates the flyback circuit during Mode 6. The time interval for this mode is relatively small due to the small sizes of output capacitors.

Equations (3-22) and (3-23) represent the differential equations for this mode, and the solution is given in equations (3-24) and (3-25). (3-24) represents the voltage across output capacitance of the switches, and (3-25) gives the current through the leakage inductance.

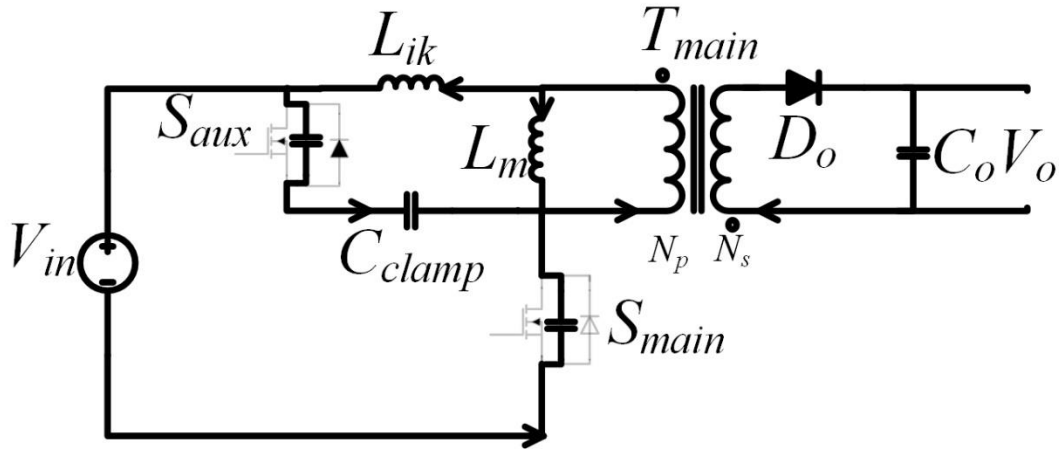

Fig. 3.7 Mode 6 ($t_5<t<t_6$)

$$v_{in} + L_{ik}\, C_r \frac{d^2 v_{c_r}}{dt^2} + n\, v_o + v_{Cr} = 0 \quad (3\text{-}22)$$

$$i_{c_r} = c_r \frac{dv_{c_r}(t)}{dt} \quad (3\text{-}23)$$

$$v_{Cr}(t) = v_{in} + n\, v_o - \left(v_{in} + n * v_o - v_{Cr}(t_5)\right)\cos(\omega_4 t) + i_{L_{ik}}(t_5) Z_4 \sin(\omega_4 t) \quad (3\text{-}24)$$

$$I_{L_{ik}}(t) = i_{l_{ik}}(t_5) * \cos(\omega_4\, t) + (v_{in} + n v_o - v_{Cr}(t_5))/Z_4 * \cos(\omega_4 t)) \quad (3\text{-}25)$$

where:

$$Z_4 = \sqrt{\frac{L_{ik}}{c_r}} \quad (3\text{-}26)$$

$$\omega_4 = \frac{1}{\sqrt{c_r . (L_{ik})}} \quad (3\text{-}27)$$

Mode 7($t_6 < t < t_7$):

At time t_6, the output capacitor of the main switch is fully discharged and its body diode starts to conduct. The main switch can be turned on during this mode with ZVS. On the other hand, the output capacitor of the auxiliary switch is fully charged, and it is completely off during this mode. Fig. 3.8 illustrates the flyback circuit during Mode 7.

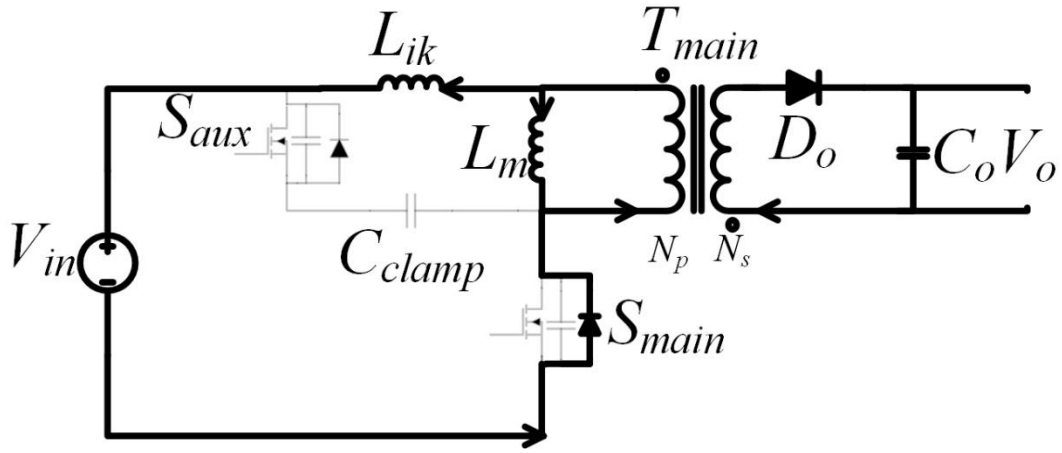

Fig. 3.8 Mode 7 ($t_6<t<t_7$)

Equations (3-28) and (3-29) represent the differential equations for this mode. Equation (3-30) represents the current through the magnetizing inductance. Equation (3-31) represents the current through the output rectifier. The clamp capacitor has a constant current and voltage during this mode, and they are shown in equations (3-32) and (3-33) respectively.

$$L_m \frac{di_{L_m}(t)}{dt} = nv_o \quad (3\text{-}28)$$

$$\frac{di_{D_{o1}}}{dt} = -n * \left(\frac{n\, v_o}{L_m} + \frac{v_{in} + nv_0}{L_{ik}}\right) \quad (3\text{-}29)$$

$$i_{L_m}(t) = i_{L_m}(t_6) - \frac{n\, v_o}{L_m} t \quad (3\text{-}30)$$

$$i_{D_{o1}}(t) = -n * \left(\frac{n\, v_o}{L_m} + \frac{v_{in} + nv_0}{L_{ik}}\right) t + i_{D_{o1}}(t_6) \quad (3\text{-}31)$$

$$i_{clamp}(t) = 0 \quad (3\text{-}32)$$

$$v_{clamp}(t) = nv_o \quad (3\text{-}33)$$

Mode 8($t_7 < t < t_8$):

This interval starts when the main switch is turned on. The current in the secondary side turns off after a very short time of turning the main switch on, and this mode ends. Fig. 3.9 illustrates the flyback circuit during Mode 8.

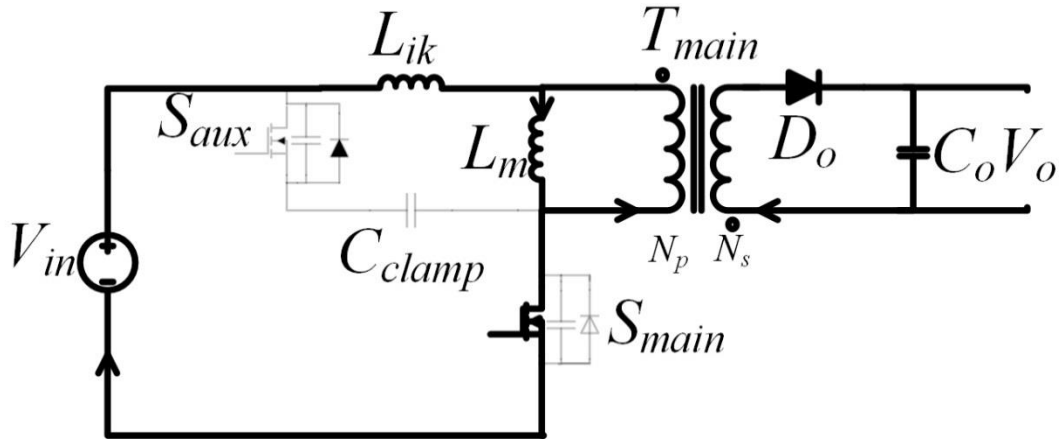

Fig. 3.9 Mode 8 ($t_7<t<t_8$)

The voltage across the primary side is equal to the reverse output voltage as shown in equation (3-34). The output capacitor of the main switch is fully discharged as shown in equation (3-35), and the voltage across the main switch is equal to zero because it is conducting current.

The snubber circuit is idle during this mode. The clamp capacitor has a constant voltage and zero current as shown in equation (3-36) and (3-37).

Currents through the leakage inductance and the magnetizing inductance are given in equations (3-38), and (3-39) respectively.

$$v_{pri}(t) = -nv_o \quad (3\text{-}34)$$

$$v_{cr,main}(t) = 0 \quad (3\text{-}35)$$

$$v_{clamp}(t) = n\, v_o \quad (3\text{-}36)$$

$$i_{clamp(t)} = 0 \quad (3\text{-}37)$$

$$i_{L_{ik}}(t) = i_{L_{ik}}(t_7) + \frac{v_{in} + n * v_o}{L_{ik}}\,(t - t_7) \quad (3\text{-}38)$$

$$i_{L_m}(t) = i_{L_m}(t_7) + \frac{n * v_o}{L_m}\,(t - t_7) \quad (3\text{-}39)$$

3.3 Design procedure:

The equations for the modes of operation that were shown in the previous section can be used to generate graphs of steady-state characteristic curves for this converter.

The program can be implemented by a computer program such as C or MATLB. In the steady-state , the current and voltage of any converter component at the start of a switching cycle must be the same as that at the end of the switching cycle. If the equations presented in the previous section are used by a program to track component

current and voltage values throughout a switching cycle when the converter is operating with a given set of component values, then the program can determine if the converter is operating in the steady-state. Once this has been determined, then the appropriate steady-state component voltage and current values can be found. If this has been done for a number of component value sets, then characteristic curves and graphs can be generated.

The characteristic graphs that are generated and showed the effects that changing a particular component value can have on converter voltages and currents. With these graphs, it is possible to proceed systematically for with design of the converter that would allow appropriate converter component values to be selected.

The range of the input voltage is between 36 volts and 72 volts. The output voltage is constant at 12 volts. The output power is between 9 Watts and 100 Watts. These values are identical to the values used in designing the flyback converter with the regenerative snubber. The aim is to maintain the same values wherever possible. By doing this, a direct comparison can be performed.

There are many parameters that need to be determined during the design. Some of these parameters need to be assumed, and they will be given values identical for those in Chapter 2. Design curves and derivations will be used to choose the rest of the converter parameters.

In this section, several guidelines that should be considered in the design of the flyback converter with the active clamp circuit shown in Fig. 3.1 are discussed. It should be noted that any design procedure that takes into account the following design considerations is iterative and thus several iterations are required before an appropriate design is selected.

1) Select the value of maximum duty cycle

The maximum duty cycle will be chosen to be 50%, the same as in the regenerative snubber circuit, in order to reduce the voltage across the main switch and the current in the output rectifier.

2) Select magnetizing inductance for flyback transformer:

Similar to the regenerative snubber, the presence of the active clamp circuit will not significantly affect the current through the primary side of the transformer.

The magnetizing inductance can be calculated using equation (3-40), which represents the rate of change for the current through an inductor:

$$\frac{\Delta \mathrm{I_{L_M}}}{\Delta \mathrm{t}} = \frac{V_{in,min} - V_{Rds,on}}{\mathrm{Lm}} \tag{3-40}$$

where $\Delta \mathrm{I_{L_M}}$ is the ripple current in the primary, $V_{Rds,on}$ is the voltage drop across the switch when the switch is in on-state and its value is around 1 Volt.

By inserting the following values into equation (3.40):

$\Delta I_{L_m} = 1$ amp;

10^{-5} seconds$\Delta \mathrm{t} = \frac{1}{f_{\mathrm{sw}}} * \mathrm{D}_{max} = \frac{1}{50000} * .5 = 1 *$

where f_{sw} is the switching frequency, and D_{max} is the maximum duty cycle , L_m can be calculated, and it was found to be L_m=0.35 mH.

3) Choosing transformer turns ratio

A transformer in an active clamp is different than a transformer in the regenerative snubber in terms of the number of windings. The active clamp circuit has two windings, which are the primary winding and the secondary winding, while the transformer in the energy regenerative snubber has three windings: the primary, secondary, and tertiary windings. Determining the turns ratio of the transformer between the primary and secondary winding will be exactly the same for both the active clamp and regenerative snubber. The design of the transformer in the active clamp circuit is easier because there is no need to choose a proper value for the number of turns for the tertiary winding. The following equation, which represents the conversion ratio for the basic flyback converter, was used to calculate the value of n_s:

$$\frac{1}{\mathrm{ns}} = \frac{V_{in,min} - V_{Rds,on}}{\mathrm{V_o} + \mathrm{V_{fw}}} * \frac{\mathrm{D_{max}}}{1 - \mathrm{D_{max}}} \tag{3-41}$$

By using the following values $V_{in,min} = 36\mathrm{v}$, $V_{Rds,on} = 1\mathrm{v}$, $V_o = 12v$, $\mathrm{V_{fw}} = .7v$, ns will be equal to 0.37.

4) Selecting leakage inductance

The value of leakage inductance for any transformer is a small percentage of magnetizing inductance. In the regenerative snubber circuit it is always better for the value of leakage inductance to be very small. On the other hand, in the active clamp circuit, it may be necessary to increase the value of leakage inductance in order to get ZVS. Increasing the value of leakage inductance can be achieved by adding an inductor on the series with the transformer.

The condition for ZVS is that the energy in leakage inductance at t_1 or t_5 should be bigger than the energy in the output capacitor [20-21]. Equations (3-42), (3-43) show the energy in leakage inductance and output capacitor respectively. Equation (3-44) shows the condition for ZVS.

$$E_{L_{ik}} = L_{ik} I_{smain,peak}{}^2 \tag{3-42}$$

$$E_{c_r} = c_r \left(v_{in,max} + n\, v_o\right)^2 \tag{3-43}$$

$$L_{ik} > \frac{c_r \left(v_{in,max} + n_s\, v_o\right)^2}{I_{smain,peak}{}^2} \tag{3-44}$$

C_r represents the value of parasite capacitor of the two switches together. This value depends on the type of the transistor that will be used. The leakage inductance was measured to be 10 µH as mentioned in Chapter 2. The required leakage inductance is 35 µH; therefore, there is a need to connect an inductor on series with the transformer. The value of the external inductor should be 25 µH.

5) Select clamp capacitor C_{clamp}

The clamp capacitor is an important factor in designing the active clamp circuit. It should be chosen properly to provide a better working condition.

In this design, the design curves method will be used to determine the value of the clamp capacitor. Fig. 3.10 shows the current passes through the clamp capacitor in Mode 4 and Mode 5. These curves were drawn with different values of the clamp capacitor. At the end of Mode 5, the current should be negative.

It is noticeable that when C_{clamp}=15 nF, the resonance frequency between the clamp capacitor and the leakage inductor is relatively high. This causes ringing across the

auxiliary switch. The smaller the value of the clamp capacitor, the higher the ringing; therefore, clamp capacitor values of less than 80 nF should be avoided.

At the end of Mode 5, the current should be negative and big enough to ensure a complete discharge of the output capacitor. Thus, setting the value of the clamp capacitor to less than 100 nF should be avoided.

All the curves that end inside the circular area can provide ZVS for both switches. All values of the clamp capacitor that are higher than 100 nF will provide ZVS. However, using large clamp capacitor values does not provide better clamping performance; it just increases cost and size. Therefore, clamp capacitor values larger than 200 nF should not be used.

Because clamp capacitors with values between 125 nF and 180 nF can be used, a 150 nf clamp capacitor will be used. Therefore, the clamp capacitor will be the same for the two topologies, the active clamp circuit and the regenerative snubber circuit.

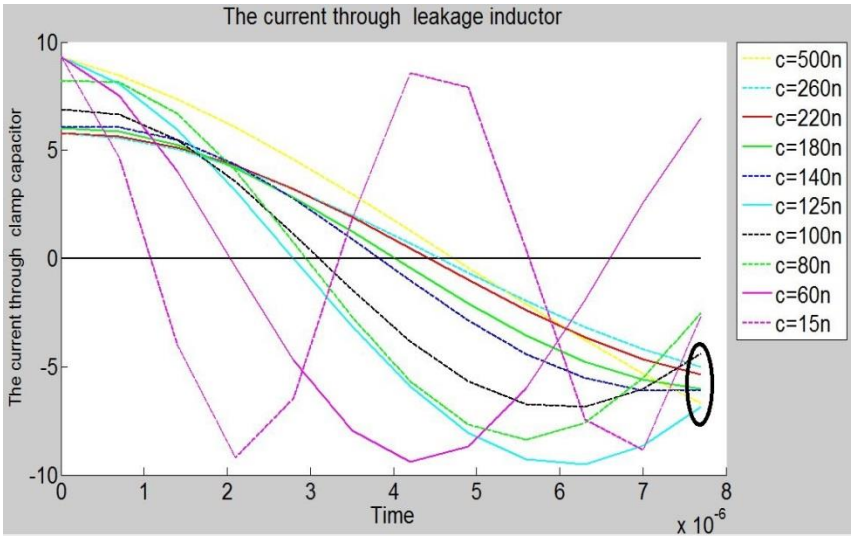

Fig. 3.10 The current through clamp capacitor for different values of clamp capacitor.

6) Select the main switch

The maximum voltage across the main switch is shown in equation (3-45) [21], The current in main switch can be calculated by using (3-46) [21].

$$v_{main,max} = v_{in,max} + v_o/n_s + i_{lik}(t_3)\, Z_3 \qquad (3\text{-}45)$$

$$I_{main,max} = \frac{P_o}{\eta\, v_{in,min}\, D_{max}} + \frac{v_{in,min}}{L_m}\, D_{max} T_{sw} \qquad (3\text{-}46)$$

By using $v_{in,max} = 72v, v_o/n_s = 32.4v,\ i_{lik}(t_3) = 6.7A, Z_2 = 15.3\ ohm$, it can be found that $v_{main,max} = 207v$,

By using $P_o = 100w,\ \eta = 0.8, L_m = 0.35, T_{sw} = 20\ us$ it can be found that $I_{main,max} = 8\ amp.$

Because one switch will be used for the two topologies, a direct comparison can be performed. The maximum current and voltage of the main switch will be determined for both topologies, and then the main switch rating will be chosen according to the maximum current and voltage for both topologies. More details will be provided in Chapter 4 about choosing the proper main switch.

7) Selecting the auxiliary switch

The body diode of the auxiliary switch conducts the current for half the period, and the channel of the MOSFET conducts the current for the rest of the period. The current in the auxiliary switch is identical to the current in the clamp capacitor. The maximum voltage stress across the auxiliary switch can be approximately calculated using equation (3-47) [20]. Equation (3-47) shows that maximum voltage across the auxiliary switch is almost equal to the sum of maximum input voltage, the reflected output voltage, and some transient voltage.

$$\mathrm{v_{aux,max}} \approx \mathrm{v_{in,max}} + \frac{v_o}{n_s} + \frac{2\mathrm{L_{ik}f_{sw}P_{o,max}}}{\eta\, \mathrm{v_{in,max}D_{max}(1 - D_{max})}} \qquad (3\text{-}47)$$

By using $v_{in,max} = 72v, \frac{v_o}{n_s} = \frac{12}{0.37} = 32.43v, L_{ik} = 35\ uH,$

$f_{sw} = 50\ Khz,\ P_{o,max} = 100w, \eta = 0.8\ , D_{\max} = 0.5, v_{aux,max} = 128.7\ volt$

The maximum current flows through the auxiliary switch is approximately equal to the maximum current through the main switch.

8) Select output rectifier:

The maximum reverse voltage across the output rectifier can be calculated by using equation (3-48), which shows that it is equal to the primary voltage reflected in the secondary side, and the output voltage. The maximum forward current can be approximately calculated using equation (3-49).

$$v_{D_{1,max}} = v_{in,max} ns + v_o \quad (3\text{-}48)$$

$$I_{D_{1,max}} \approx \frac{2P_o}{v_o(1 - D_{max})} \quad (3\text{-}49)$$

By using $v_{in,max} = 72v$, $ns = 0.37$, $v_o = 12v$, it can be found that $v_{D1,max} = 38.64v$. By using $P_o = 100w$, it can be found that $I_{D_{1,max}}$ is equal to 33.33 Amp. The mechanism that will be used to choose the output rectifier is similar to the one used choosing the main switch. The maximum current and voltage of the output rectifier for both topologies will be determined, and then ratings will be chosen according to the two topologies. The same output rectifier will be used for the two topologies, so a direct comparison can be performed.

9) Select output capacitor:

The output capacitor is the same for both topologies, the active clamp and the regenerative snubber. The equations and description on how to choose the output capacitor were shown in chapter 2.

Fig. 3.11 shows the designed Flyback converter with the active clamp technique.

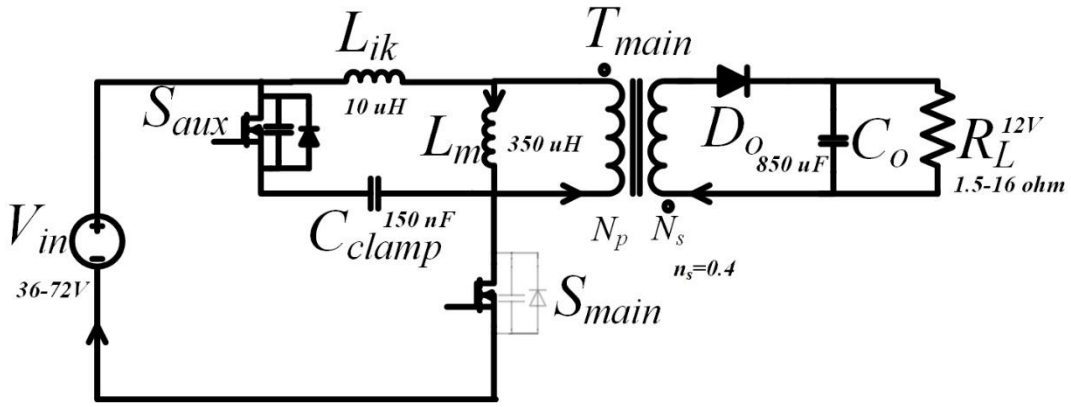

Fig. 3.11 Designed flyback converter with active clamp technique

Chapter 4 will give complete details about the type of component used in the building of the converter.

3.4 Conclusion

In this chapter, the operation, analysis, and design of a flyback converter with an active clamp snubber were presented. The general operation and the converter's modes of operation of the converter were explained, equations that define the operation of the converter for each operation mode were derived, and these equations were used to develop a procedure for the design of the converter. Based on the analysis and design, the following characteristics were determined:

A) When the clamp capacitor is smaller than 80nF, then the auxiliary switch will suffer from higher ringing.

B) If the clamp capacitor is higher than 100nF, then ZVS will be achieved.

The design procedure was demonstrated with an example for the design of a converter with input voltage V_{in} = 36-72 Volts, output voltage V_o = 12 Volts, maximum output power $P_{o.max}$ = 100 Watts, and switching frequency f_{sw} = 50 kHz. Based on the design example, the values of certain key converter parameters were obtained and these parameter values were used to build a converter prototype that was used to obtain the experimental results that will be described in Chapter 4.

Chapter 4

4 Experimental Results

4.1 Introduction

In this chapter, results obtained from experimental prototypes of the flyback converter with the regenerative energy snubber and the active clamp converter are presented. Two prototype types were built for each converter topology: a low input voltage prototype with input voltage range of 36-72 VDC and a high input voltage prototype with input voltage range 200 – 400 VDC. All the prototypes were built to supply a maximum output power of 100 W and an output voltage of 12 Volts. The converter switching frequency for all the prototypes was 50 kHz.

The low input voltage range is representative of applications such as telecom. where the input voltage can be a DC battery that can range from 36 V to 72 V, or solar energy power systems, where the input voltage can range from 30 V to 40 V. The high input voltage range is representative of applications where a flyback converter is the second converter of a two-stage AC-DC power converter that consists of an AC-DC front-end converter feeding the input of a DC-DC flyback converter such as the two converters studied in this work.

Efficiency measurements of two sets of two converter topologies are presented in this chapter. The first set includes efficiency measurements of a low input voltage flyback converter with a regenerative energy snubber and a low input voltage active clamp converter; the second set includes efficiency measurements of a high input voltage flyback converter with a regenerative energy snubber and a high input voltage active clamp converter. Based on these measurements, conclusions about the performance of the two converter topologies are made at the end of the chapter.

4.2 Experimental Results

Circuit diagrams of a flyback converter with regenerative energy snubber and an active clamp flyback converter are shown in Fig. 4.1 and 4.2 respectively. The

component values used in the converter prototypes are listed in Table I. Figs. 4.3-4.9 show typical experimental waveforms obtained from the prototypes of the two converter types.

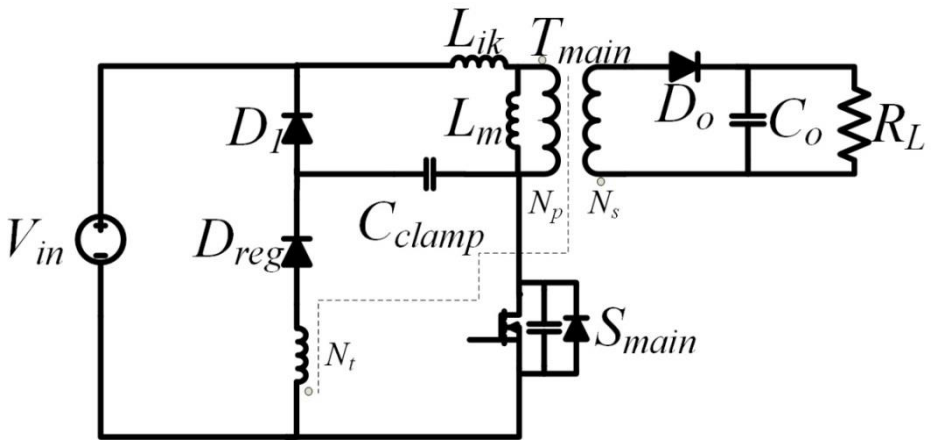

Fig. 4.1 Regenerative snubber circuit.

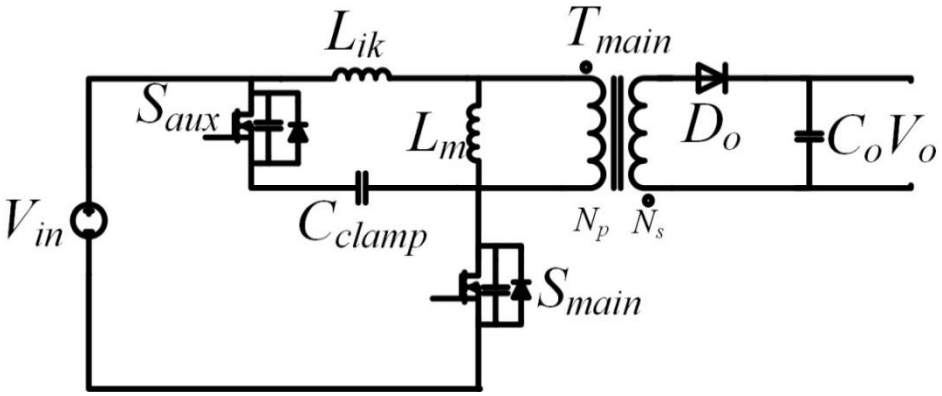

Fig. 4.2 Active clamp circuit.

TABLE I. List of converter prototype components.

	Flyback converter with energy regenerative snubber	Active clamp flyback converter
Main Switch	FQP22N30	FQP22N30
Auxiliary switch	-	FPQ22N30
Clamp capacitor	C340C154K2R5TA	C340C154K2R5TA
Output diode	APT30S20B(G)	APT30S20B(G)
Output capacitor	Nichicon UVY1H102MHD	Nichicon UVY1H102MHD

Transformer	ETD44 with Np:Ns:Nt = 4:1:1.5	ETD44 with Np:Ns = 4:1
D_1	FML-G22S	-
D_{reg}	12TQ150	-

Table I. List of converter prototype components.

Fig. 4.3 shows the switch gating signal, the voltage across the switch, and the current through the switch of the flyback converter with the regenerative energy snubber. It can be seen that the switch does not have any voltage spikes; this is because the clamp capacitor in the snubber is effective in suppressing such spikes. It can also be seen that the switch current has a small resonant hump around the time when the switch has just been turned on; this is because of the clamp capacitor discharging through the switch and the tertiary winding.

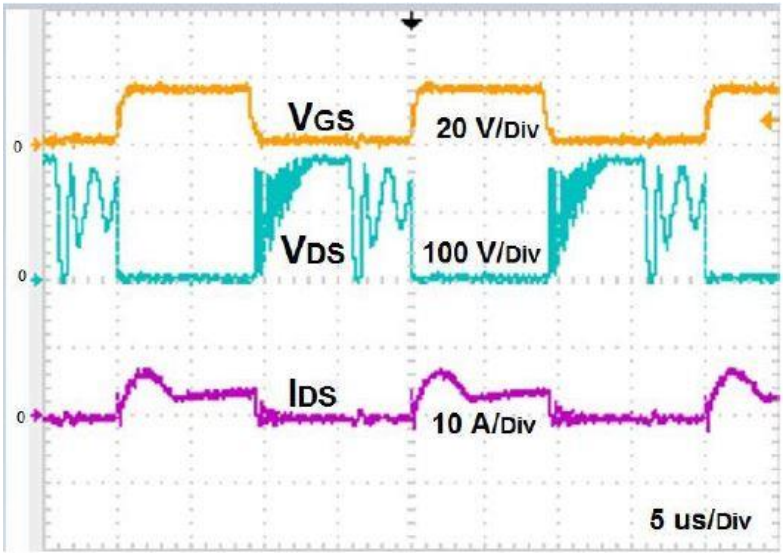

Fig. 4.3. Switch gating signal V_{gs}, switch voltage V_{ds}, and switch current I_{ds} of the flyback converter with regenerative passive snubber when V_{in}=72 V, V_{out}=12 V, P_{out}=72 W (V_{gs}: 20 v/div; V_{ds}: 100 v/div; I_{ds}: 10A/div.)

Fig. 4.4 shows the gating signals of the main switch, the voltage across the clamp capacitor, and the current through the tertiary winding of the flyback converter with the regenerative energy snubber. From this figure, it can be seen that the voltage across the clamp capacitor rises when the switch is turned off and falls when the switch is turned on. It can also be seen that the fall in capacitor voltage occurs when there is current flowing in the tertiary winding. It should be noted that the current in

the winding is a hump, which shows the resonant interaction between the clamp capacitor and the inductance of the tertiary winding. Moreover, this hump of current exists for only a small fraction of the switching cycle.

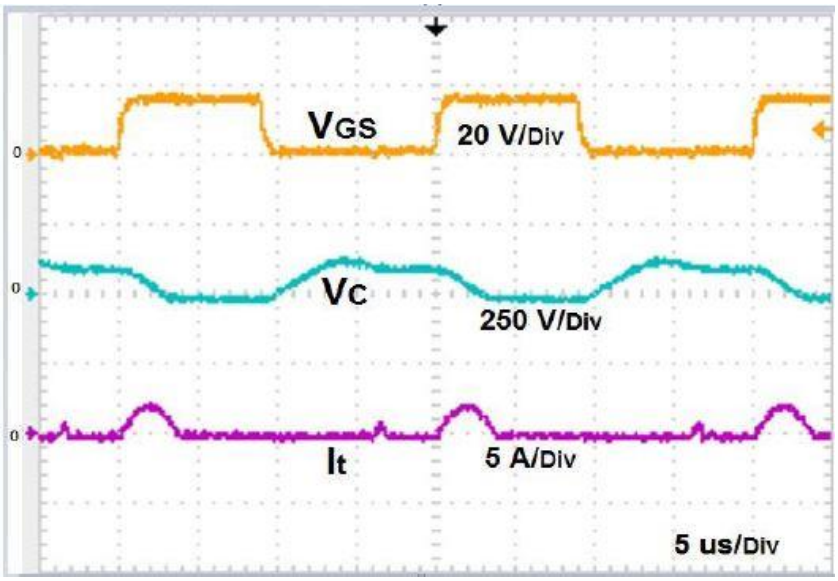

Fig. 4.4 Main switch gate signal V_{gs}, clamp capacitor V_c , and current through tertiary winding I_{Dreg} of the flyback converter with regenerative passive snubber when V_{in}=72 V, V_{out}=12 V, P_{out}=72 W (Vgs : 20v/Div; Vc : 250v/Div; I_{Dreg} :10A/Div)

Fig. 4.5 shows the switch gating signal and the current through the output diode of the flyback converter with the regenerative energy snubber. It can be seen that current flows through the output diode only when the switch is off, as is expected of a flyback converter. It can also be seen that the output diode current has no reverse recovery current; this is because a fast recovery diode was used at the output.

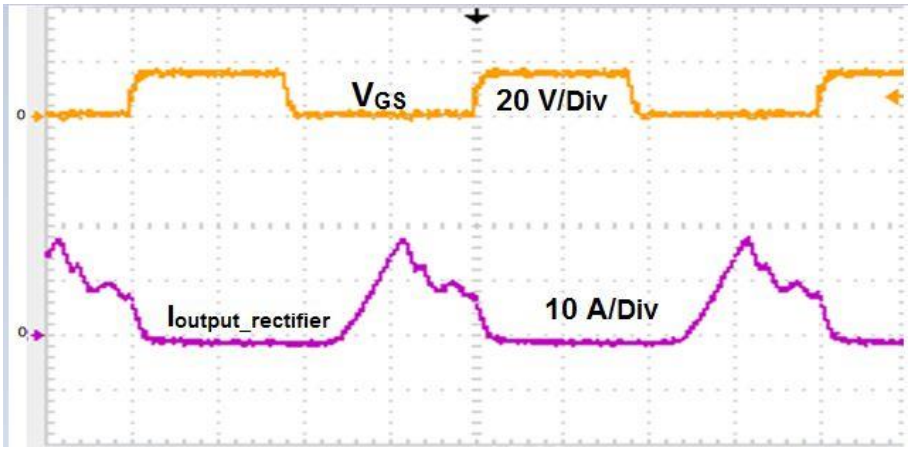

Fig. 4.5 Main switch gate signal V_{gs}, current through output rectifier I_{D1} of the flyback converter with regenerative passive snubber when V_{in}=72 V, V_{out}=12 V, P_{out}t=72 W (Vgs : 20v/Div; I_{D1} :10A/Div)

Fig. 4.6 shows the main switch gating signal, voltage and current of the active clamp flyback converter. It can be seen that the voltage across the main switch drops to zero before it is turned on so that it can turn on with zero-voltage switching (ZVS) and thus with reduced switching losses. It can also be seen that the current in the switch is negative just before it is turned on. This is because current is flowing through the body diode of the switch at this time, thus forcing the voltage across the switch to be zero. Having current flowing through the switch at this time is the main mechanism by which the main switch can be made to operate with ZVS.

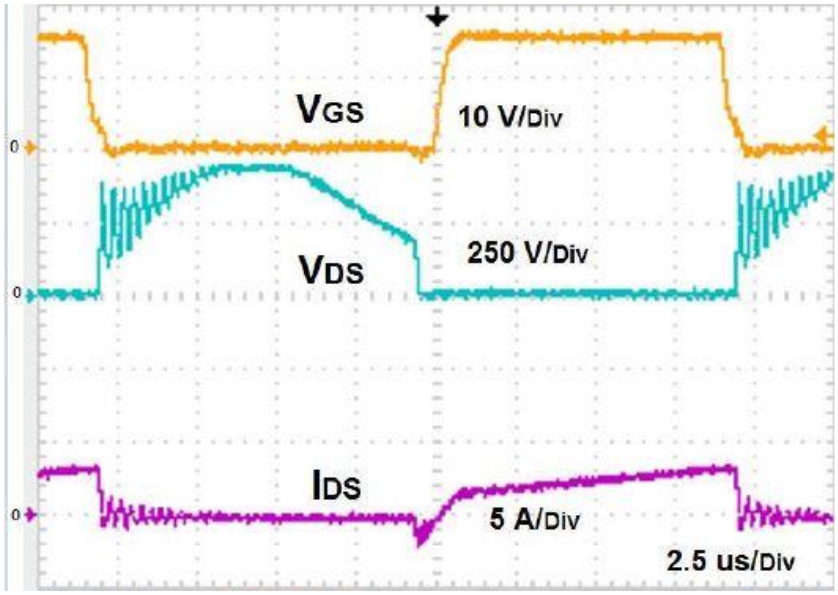

Fig. 4.6 Main switch gate signal Vgs, main switch voltage Vds, and main switch current Ids of the flyback converter with active clamp circuit when V_{in}=72 V, V_{out}=12 V, P_{out}t=72 W (Vgs : 10v/Div; Vds : 100v/Div; Ids :5A/Div)

Fig. 4.7 shows the gating signal of the auxiliary switch, the voltage across this switch and the current flowing through it. It can be seen that the auxiliary switch operates with ZVS as it is turned on when current is flowing through its body diode (the negative part of the switch current waveform).

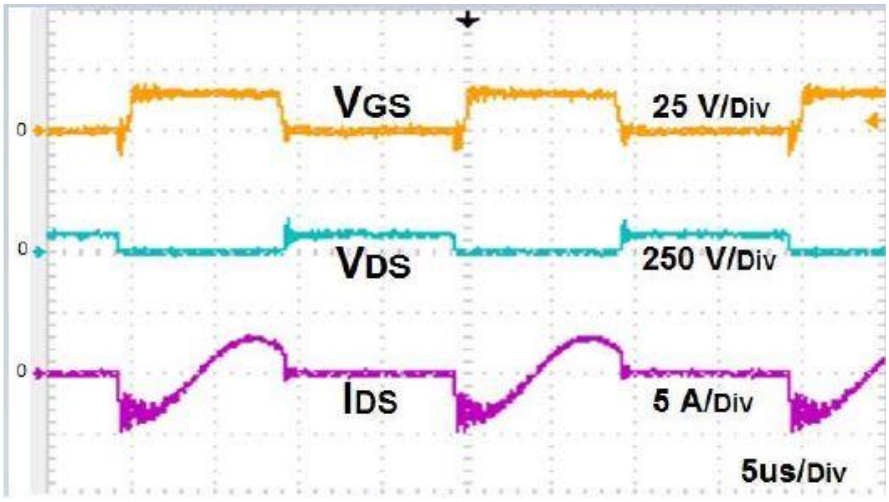

Fig. 4.7 Auxiliary switch gate signal Vgs, auxiliary switch voltage Vds, and auxiliary switch current Ids of the flyback converter with active clamp circuit when V_{in}=72 V, V_{out}=12 V, P_{out}=72 W (Vgs : 20v/Div; Vds : 250v/Div; Ids :5A/Div)

Fig. 4.8 shows the switch gating signal and the current through the output diode of the active clamp flyback converter. It can be seen that current flows through the output diode only when the switch is off, as is expected of a flyback converter. It can also be seen that the output diode current has no reverse recovery current; this is because a fast recovery diode was used at the output.

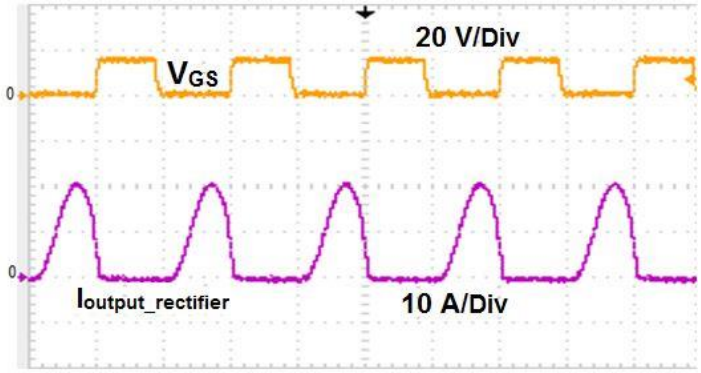

Fig. 4.8 Main switch gate signal Vgs, the current through the output rectifier of the flyback converter with with active clamp circuit when V_{in}=72 V, V_{out}=12 V, P_{out}=72 W (Vgs : 20v/Div; I_{D1} :10A/Div)

Fig. 4.9 shows that the voltage across the clamp capacitor of the active clamp converter. It can be seen that it has the shape of a resonant hump. This is because of the interaction between the clamp capacitor and the primary-side inductance of the

transformer. It can also be seen that the current in the capacitor does not begin to rise until the switch is turned off; this is because current flows in the switch when it is on.

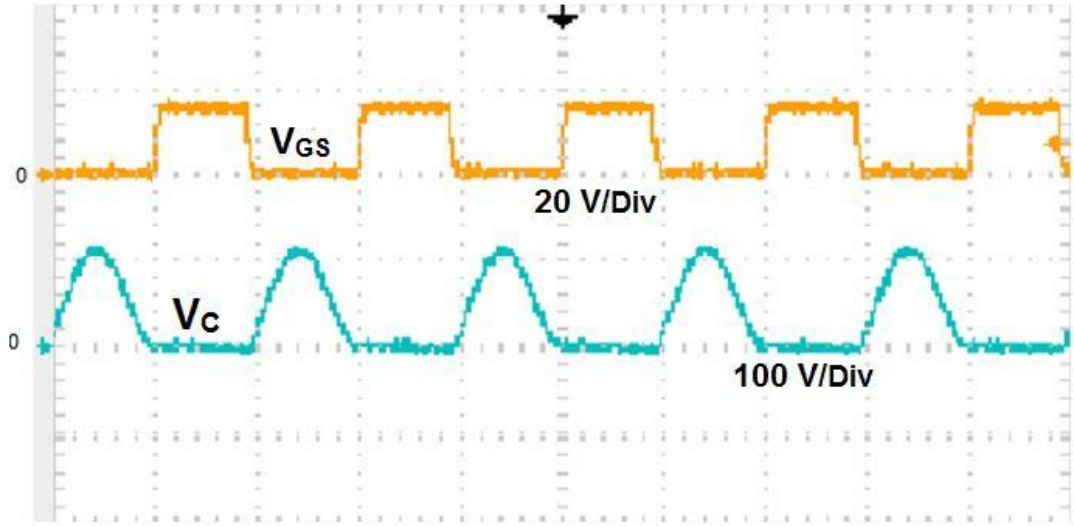

Fig. 4.9 Main switch gate signal Vgs, clamp capacitor Vc of the flyback converter with with active clamp circuit when V_{in}=72 V, V_{out}=12 V, P_{out}=72 W (Vgs : 20v/Div; Vc : 100v/Div)

4.3 Efficiency Comparison

In this section, the efficiency of a flyback converter with the regenerative energy snubber is compared to that of an active clamp converter. The comparison is made for two input voltage ranges: a low input voltage range of 36-72 VDC and a high input voltage range of 200 -400 VDC. The output voltage of the converter prototypes used in the comparison was 12 VDC, the maximum output power was 100 W and the converter switching frequency was 50 kHz.

Fig. 4.10 shows graphs of converter efficiency vs output power for both flyback converter topologies at three different input voltages in the low input voltage range: 36, 54, and 72 V. Fig. 4.11 shows graphs of converter efficiency vs output power for both flyback converter topologies at three different input voltages in the high input voltage range: 200, 311, and 376 V.

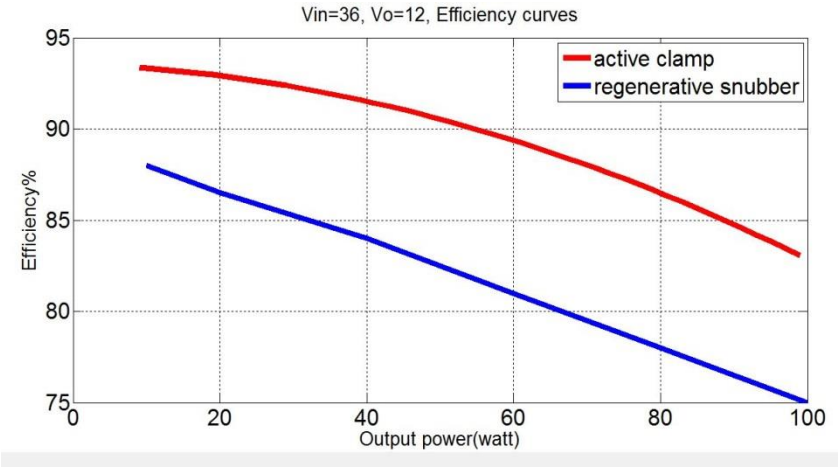

(a)

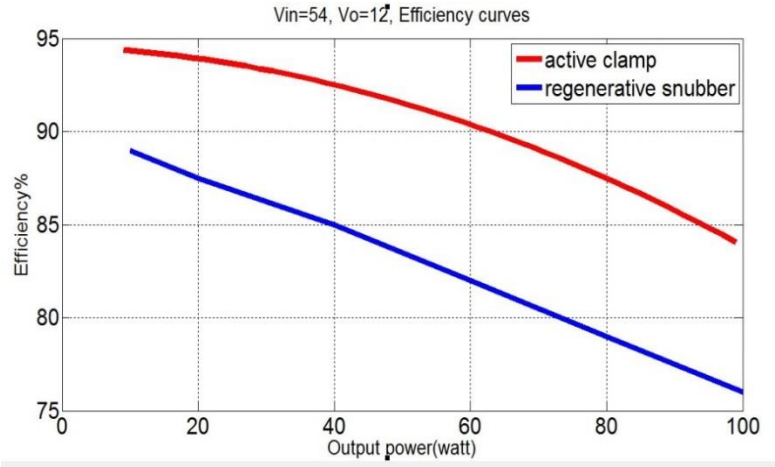

(b)

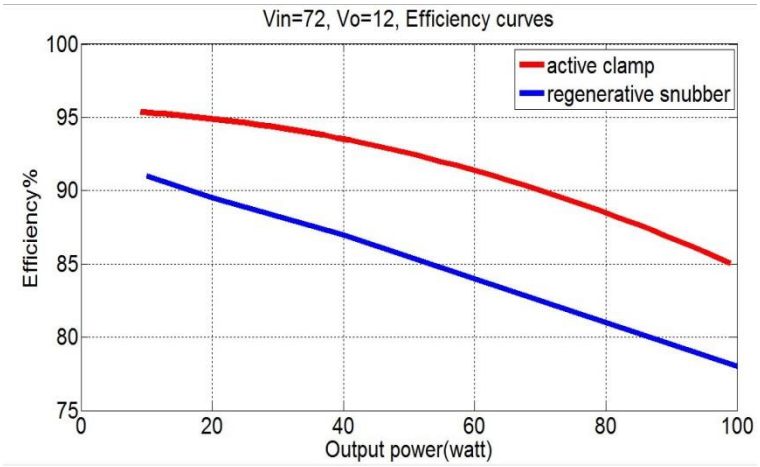

(c)

Fig. 4.10 Efficiency curves for both topology (Active clamp and regenerative snubber circuit) at three different cases ((a):Vin=36v, (b): Vin=54v, and (c): Vin=72v), The converter rating is 100 W.

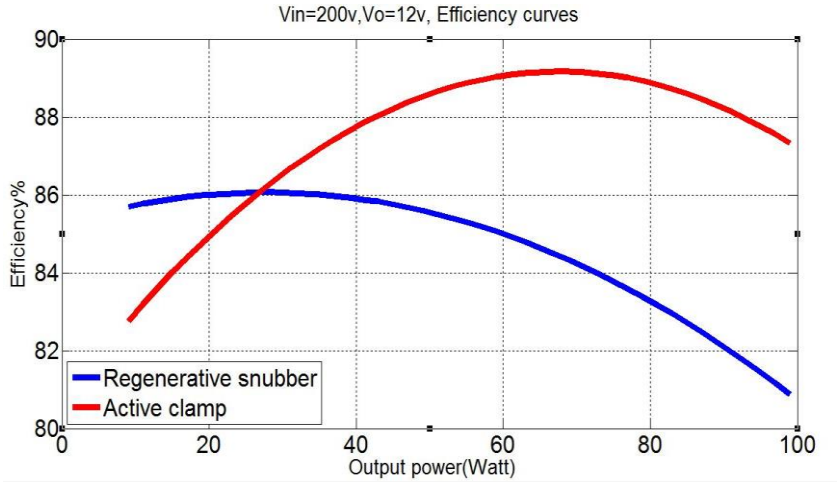

(a)

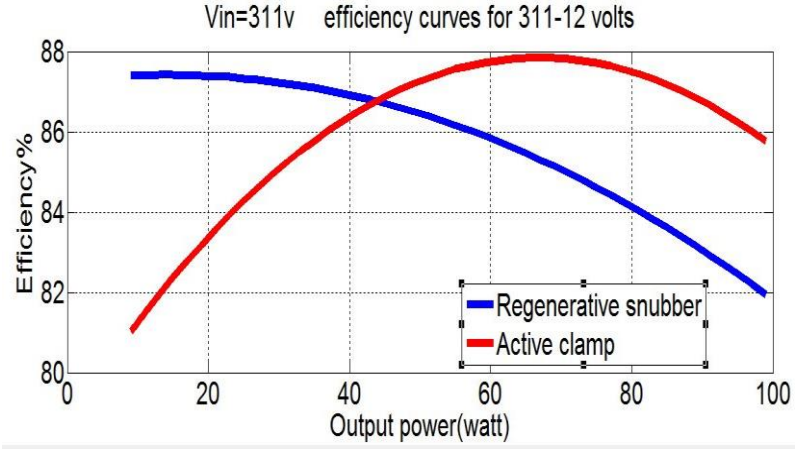

(b)

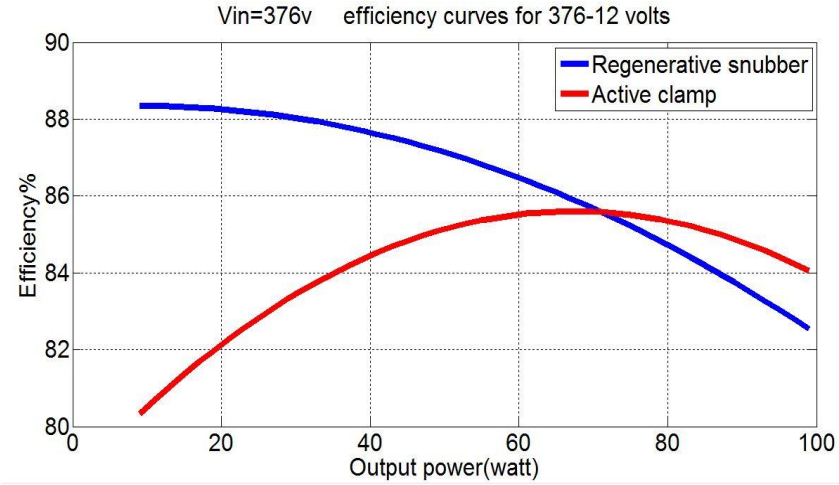

(c)

Fig. 4.11 Efficiency curves for both topology (Active clamp and regenerative snubber circuit) at three different cases((a):Vin=200v, (b): Vin=311v, and (c): Vin=376v), The converter rating is 100 W.

The following conclusions can be made based on the graphs of converter efficiency vs output power shown in Fig. 4.10 and 4.11:

- When the two converters are operating with an input voltage in the low input voltage range, the active clamp converter is always more efficient than the flyback converter with the regenerative energy snubber.

- When the two converters are operating with an input voltage in the high input voltage range, the flyback converter with the regenerative energy snubber is more efficient than the active clamp converter except when the two converters are operating with heavy loads.

- In general, the flyback converter with regenerative energy snubber is the more efficient converter when the input current (and thus the transformer primary current) is low and is the less efficient converter when the input current (and transformer primary current) is high.

The efficiency results shown in Fig. 4.10 and 4.11 can be explained by noting that the active clamp converter loses its ZVS capability when the transformer primary current is low. When this current is low, there is not enough energy to discharge the output capacitance of the main converter switch so that when the switch is turned on, it does so with voltage across it and thus with switching losses. Given that the converter with the regenerative snubber has switching losses but does not have an auxiliary circuit that has losses as well, this converter will be more efficient than the active clamp converter. It is only when the active clamp converter operates with ZVS that the savings in switching losses exceeds the losses of the auxiliary circuit so that the active clamp converter becomes the more efficient converter.

4.4 Cost comparison

In this section, a comparison between the two snubbers are done in terms of cost. Table II shows a comparison between the cost in components that are not the same for both topologies. In this schedule, the price of components that are not the same for both topologies is only presented. The main switch does not affect the cost comparison because it is found in both topologies, and exactly same transistor was used for both topologies. Five components are not the same for both topologies. The

auxiliary switch is found only in the active clamp circuit, and it costs around 3.44$. The diodes D_1, D_{reg} are found only in the energy regenerative snubber, and they cost 2.12$ and 0.95$ respectively. The transformer costs approximately 3$ in this prototype for active clamp circuit. The other transformer in energy regenerative snubber, which is three winding transformer, is more expensive than the transformer in active clamp topology around 15%. It costs around 3.45$. The resonant inductor is required only in active clamp circuit, and it costs 1.5$.

Component name	Active Clamp	Energy regenerative snubber
Auxiliary switch	FQP22N30 3.44$	-
D_1	-	$2.12
D_{reg}	-	0.95$
Transformer	3$	3$ +15%=3.45 $
Resonant inductor	1.25$	-
Main Switch	Same for both topologies	Same for both topologies
Output diode	Same for both topologies	Same for both topologies
Clamp capacitor	Same for both topologies	Same for both topologies
Output capacitor	Same for both topologies	Same for both topologies

Table II Cost comparison (prices obtained during December 2017)

According to schedule II, the active clamp circuit costs 1.17$ more than what energy regenerative snubber costs. Also active clamp may require an external inductor that helps in providing ZVS, and this causes the active clamp circuit to have more space than what it is required for energy regenerative snubber.

It can be concluded that energy regenerative snubber costs less than the active snubber, and it requires less space.

4.5 Conclusion

Experimental results obtained from prototypes of the flyback converter with the regenerative energy snubber and the active clamp converter were presented in this chapter. Graphs of converter efficiency vs output power obtained from efficiency measurements were also presented as well. Based on these graphs, it was determined that the flyback converter with the regenerative energy snubber was the more efficient converter when the input current was low and was the less efficient converter when the input current was high. This was mainly because the active clamp converter can operate with ZVS when the input current is high and cannot operate with ZVS

when the input current is low. Since the active clamp converter has an auxiliary circuit that the other converter does not, the active clamp converter is the less efficient converter when the input current is low because it has switching losses and auxiliary circuit losses that the other converter does not have.

Chapter 5

5 Conclusion

5.1 Summary

DC-DC flyback converters are very popular in low power conversion application of 150 W or less as they are inexpensive and simple. The MOSFET switch in these converters, however, must be implemented with some sort of snubber to suppress high voltage spikes that can be caused by the interaction of the leakage inductance of the flyback transformer and the output capacitance of the switch. Without such a snubber, the voltage spikes that appear may have voltage levels that exceed the ratings of the device so that the end result can be a catastrophic failure of the device.

Snubbers can be generally divided into two types: passive snubbers and active snubbers. Passive snubbers consist of a clamping capacitor and various other passive elements that allow the clamping capacitor to discharge. The most efficient passive snubber is the regenerative energy snubber, which has a winding that is taken from the flyback transformer in its circuit. This winding allows energy from the leakage inductance that would otherwise be dissipated to be transferred to the output and also limits the amount of current flowing out of the snubber that circulates in the converter.

Active snubbers are like passive snubbers, but have an active switch in their circuit. The most popular type of active snubber is the active clamp snubber because of its relatively low cost, simplicity, and high efficiency. Unlike passive snubbers, active snubbers also allow the main converter switch to operate with zero-voltage switching (ZVS), thus further reducing switching losses.

In the past, passive snubbers have been considered to be less expensive, but less efficient than active snubbers, but recent improvements in the efficiency of passive snubbers have placed this general rule in doubt. To date, there has been no comparison between passive snubbers and active snubbers as it has been assumed that active snubbers are obviously more efficient. The main objective of this thesis has been to compare the performance of the regenerative energy snubber and the active clamp snubber and to see which snubber is most efficient under various input voltage

and output load conditions. Such a comparison would allow power electronics engineers to make better decisions as to which snubber to use for a given set of circumstances.

The contents of this thesis can be summarized as follows: In Chapter 1, certain fundamental principles relating to the work done in this thesis were reviewed as was the literature on passive and active snubbers for flyback converters. In Chapter 2, the general operation of the regenerative energy snubber was explained in detail as were the modes of operation that a flyback converter with such a snubber goes through during a switching cycle. These modes of operation were analyzed and the results of the analysis were used to derive a procedure for the design of the converter that was demonstrated with an example. The same was done in Chapter 3 for a flyback converter with the active clamp snubber. Experimental results obtained from converter prototypes of the two converters that have been designed according to the design procures presented in Chapters 2 and 3 were presented in Chapter 4 and a comparison of the efficiency of flyback converters with each of the two snubbers operating under various input voltage and output load conditions was made.

5.2 Conclusions

Based on the research work that was done, the following conclusions can be made:

(i) A flyback converter with an active clamp snubber is always more efficient than with a regenerative energy snubber when the input DC source voltage is 72V or lower. Applications with such a voltage source include renewable energy applications such as solar power systems and fuel cell power systems and telecom applications where power conversion from a DC bus with voltage in the range of 36V-72V is required. The reason for the greater efficiency of the active clamp flyback converter is that the main switch operates with ZVS or near ZVS through the entire load range so that turn-on switching losses are always reduced, unlike these losses in the regenerative energy snubber flyback converter.

(ii) The efficiency of a flyback converter with a regenerative snubber increases as the input voltage is increased to the point where such a converter can actually be more efficient than that the active clamp converter under high input DC source voltage conditions and medium to light loads. This is especially true when the input voltage is

400 V, which is a typical input voltage that occurs when a flyback converter is implemented as the back-end converter in a two-stage AC-DC converter with an AC-DC front-end converter stage. AC-DC is used in different applications where the input voltage is AC and the required voltage is DC include cell phone chargers and personal computers. The reason for this greater efficiency is that under high voltage conditions, the active clamp converter loses its ability to operate with ZVS so that it becomes more like the regenerative energy converter, but with greater losses due to the switching losses of its active clamp switch.

(iii) The value of clamp capacitor is very critical especially in designing the energy regenerative snubber where it has a small range. Using values of clamp capacitor out of this range causes a degradation of the efficiency. The range of clamp capacitor values in the active clamp technique is less critical where it has a wider range.

5.3 Contribution

The main contribution of this thesis is that this is the first time, to the best of the author's knowledge, that a comparison has been made between the efficiency of a flyback converter with a regenerative energy snubber, which is considered to be the best passive snubber, and the active clamp snubber, which is considered to be the best active snubber. In some cases, the experimental results that were obtained as part of this work contradict the general belief that active snubbers are always more efficient than passive snubbers regardless of the application. The comparison presented in this thesis will allow power electronics engineers to make better decisions as to which type of snubber should be used for a particular application.

References:

[1] G. Koo, " Design guidelines for RCD snubber of flyback converters," Fairchild Semiconductor Corporation 2006.

[2] S. Finney, B. Williams, and T. Green, "RCD snubber revisited," *IEEE Transaction on industry applications,* VOL.32, NO.1, pp. 155-160 , January/February 1996.

[3] P. Meng, H. Chen, S. Zheng, X. Wu, and Z. Qian, "Optimal design for the damping resistor in RCD-R Snubber to suppress Common-mode Noise," *Applied Power Electronics Conference and Exposition (APEC)* 2010, pp. 691-695.

[4] P. Meng, X. Wu, J. Yang, H. Chen, and Z. Qian, "Analysis and design considerations for EMI and losses of RCD snubber in Flyback converter," *Applied Power Electronics Conference and Exposition (APEC)* 2010, pp. 642-647.

[5] W. McMurray, "Selection of snubbers and clamps to optimize the design of transistor switching converters," *IEEE Power Electronics Specialists Conference* 1979, pp. 62-74.

[6] A. Hren, J. Korelic, and M. Milanovic, "RC-RCD clamp circuit for ringing losses reduction in a flyback converter," *IEEE Transactions on circuits and systems,* Vol.53, No.5, May 2006.

[7] S. Liu, F. Zhang, and Q. Zhang, "Optimal Design of RCD Parameters in Flyback Converter," *International Symposium on Computer, Consumer and Control,* IEEE 2016, pp. 583-586.

[8] S. Ben-Yaakov, and G. Ivensky, "Passive lossless snubbers for high frequency PWM converters," Power electronics laboratory, Department of electrical and computer engineering, Ben-Gurion University of the Negev, 1999.

[9] C. Liao, and K. Smedley, "Design of High Efficiency flyback converter with energy regenerative snubber," *Applied Power Electronics Conference and Exposition (APEC)* 2008, pp.796-800.

[10] A. Abramovitz, C. Liao, and K. Smedley, "State-plane Analysis of Regenerative Snubber for Flyback converters," *IEEE Transactions on power electronics*, Vol. 28, , No.11, pp. 5323-5332, November 2013.

[11] M. Mohammadi, and M. Ordonez, "Flyback lossless passive snubber," *IEEE Energy Conversion Congress and Exposition (ECCE)* 2015, pp. 5896-5901.

[12] A, Abramovitz, T. Cheng, and K. Smedley, "Analysis and design of forward converter with energy regenerative snubber," *IEEE Transactions on power electronics,* Vol.25, No.3, March 2010.

[13] T. Ninomiya, T. Tanaka, and K. Harada, "Analysis and Optimization of a Nondissipative LC Turn-off snubber," *IEEE Transactions on power electronics,* Vol.3, No.2, APRIL 1988.

[14] C. Wang, "A Novel ZCS-PWM Flyback Converter With a Simple ZCS-PWM Commutation Cell," *IEEE Transaction on industrial electronics,* Vol. 55, No.2, February 2008.

[15] M. Delshad, and A. Narimani, "A new Soft switching Flyback DC-DC Converter with Minimal Auxiliary Circuit Elements," Universal Journal of Electronic Engineering 2013, pp. 105-109.

[16] Y. Xi, P. Jain, and G. Joos, "A Zero Voltage Switching Flyback Converter Topology," *IEEE Power Electronics Specialists Conference* 1997, Vol.2, pp. 951 – 957.

[17] Y. Xi, P. Jain, G. Joos, and Y. Liu, “An Improved Zero Voltage Switching Flyback Converter Topology,” IEEE Power Electronics Specialists Conference *PESC 1998,* Vol.2, pp. 923-929.
[18] T. Halder, “ A comparative Study of the Hard & Soft Switching of the Flyback Converters,” *IEEE Power India International Conference (PIICON)* 2014, pp. 1-6.
[19] C. Wang, C. Su, and C. Yang, "ZVS-PWM flybak converter with a simple auxiliary circuit, " *IEE Proceedings – Electric power Applications* 2006, Vol.153, pp. 116-122.
[20] R. Watson, F. Lee, and G. Hua, “Utilization of an active-clamp circuit to achieve soft switching in flyback converters,” *IEEE Transactions on Power Electronics,* Vol.2, No. 1, pp. 162–169, Jun. 1994.
[21] B. Lin, H. Chiang, K. Chen, and D. Wang, “Analysis, design and implementation of an active clamp flyback converter,” IEEE International Conference on Power Electronics and Drives Systems *(PEDS) 2005,* Vol.1, pp. 424-429, 2005.
[22] P. Alou, O. Garcia, J. Cobos, J. Uceda, and M. Rascon, “Flyback with active clamp: A suitable topology for low power and very wide input voltage range applications,” *IEEE in Applied Power Electronics Conference and Exposition (APEC)* 2002 , Vol.1, pp. 242-248.
[23] S. Aruna, S. Srivani, and P. Balaji, “Multi output Active Clamped Flyback Converter,” *International Journal of Advanced Research in Electrical , Electronics and Instrumentation Engineering* 2014, Vol.4, No.7, pp 596-601.
[24] P. Jailyn, A. Dheeraj, and V. Rajini, “Analysis of Active Clamp FlyBack Converter,” *Modern Applied science* 2015, Vol.9, No.1, pp. 12-24.
[25] C. Choi, C. Li, and S. Kok, “Modeling of An Active Clamp Discontinuous Conduction Mode Flyback Converter under Variation of Operating Conditions,” *IEEE International Conference on Power Electronics and Drive Systems,* (PEDS) 1999, pp. 730-733.
[26] J. Kim, M. Ryu, B. Min, and E. Song, “A Method to Reduce Power Consumption of Active-Clamped Flyback Converter at No-Load condition,” *Annual Conference on IEEE Industrial Electronics IECON 2006,* pp. 2811 - 2814,
[27] J. Zhang, X. Huang, X. Wu, and Z. Qian, "A High Efficiency Flyback Converter With New Active Clamp Technique," *IEEE Transactions on Power Electronics.,* Vol.25, No.7, pp. 1775-1785, July 2010.
[28] R. Perrin, N. Quentin, B. Allard, C. Martin, and M. Ali, “High-Temperature GaN Active-Clamp Flyback Converter With Resonant Operation Mode,” *IEEE Journal of emerging and selected topics in power electronics,* Vol.4, No.3, SEP 2016.
[29] T. LaBella, B. York, and C. Hutchens and “Dead Time Optimization through Loss Analysis of an Active-Clamp Flyback Converter Utilizing GaN Devices,” *IEEE Energy Conversion Congress and Exposition (ECCE)* 2012, pp. 3882-3889
[30] X. Yoshida, T. Ishii, and N. Nagagata, "Zero voltage switching approach for flyback converter," *Telecommunications Energy Conference (INTELEC) 1992,* pp. 324-329.
[31] S. Larousse, H. Razik, R. Cellier, N. Abouchi, and P. Volay," Active Dead-time optimization for wide range Flyback active-clamp converter,"*International Exhibition and Conference for Power Electronics, Intelligent Motion, Renewable Energy and Energy Management* PCIM Europe 2016, pp. 1-6

[32] S. Yang, Z. Qian, Q. Ouyang, and F. Peng, “An improved Active-clamp ZVS Forward Converter Circuit,” *IEEE Applied Power Electronics Conference Exposition (APEC) 2008*, pp 318-322.

[33] B. Lin, C. Yang, S. Tsay, and D. Wang, “ Analysis and Implementation of an Active Clamp ZVS Forward Converter,” *IEEE International Conference on Industrial Technology 2005* , pp 1427-1432.

[34] L. Ritu, and G. Anitha, “Analysis of Utilization of Active Clamp Circuit to achieve Zero Voltage Switching in Forward Converter,” *International Conference on Advances in Recent Technologies in Communications and Computing (ARTCom 2013),* pp 446-450.

[35] E. Kim, S. Choi, and M. Kye, “ An improved Active-Clamp ZVS Forward Converter with A Lossless Snubber,” - *International Telecommunications Energy Conference (Intellect) 2009,* pp 1-4.

[36] H. Huang, “Design Guidelines on the Effect of Resonant Transitions of Forward Converter on Efficiency with Active Clamp,” *IEEE Applied Power Electronics Conference and Exposition (APEC) 2008* , pp 600-606.

[37] M. Jinno, J. Sheen, and P. Chen, “ Effects of Magnetizing Inductance on Active-clamped Forward Converters,” *Telecommunications Energy Conference,. (INTELEC) 2003,* pp. 636-642.

Curriculum Vitae

Name Adel Alganidi

Post-secondary Education and Degrees: Misurata University, Misurata, Libya
2005-2010 B.Eng.Sc

Western Univesity, London, ON
2015-2017 M.E.Sc

Honours and Awards: Outstanding performance Award, Misurata University.
Ministry of Higher Education Graduate Scholarship, Libya.

Related Work Experience Teaching assistant
Misurata University
2012-2014

Teaching assistant
Western University
2015-2017

Publication:

"Adel Alganidi, Adel Abusnina, " A novel high gain DC-DC full-bridge converter for low voltage renewable energy applications" CCECE 2017, pp. 1-4.

"Adel Alganidi, Adel Abusnina, "A Comparative Study of DC-DC Flyabck converters for Telecom Applications" INTELEC 2017.